Catalysis Today 220–222 (2014) 274–294

Contents lists available at ScienceDirect

Catalysis Today

journal homepage: www.elsevier.com/locate/cattod

A review of experimental procedures for heavy oil hydrocracking with dispersed catalyst

M.J. Angeles*, C. Leyva, J. Ancheyta, S. Ramírez

Instituto Mexicano del Petróleo, Eje Central Lázaro Cárdenas Norte 152, Mexico City, 07730, Mexico

ARTICLE INFO

Article history:
Received 28 February 2013
Received in revised form 20 August 2013
Accepted 22 August 2013
Available online 16 September 2013

Keywords:
Dispersed catalyst
Hydrocracking
Hydroconversion
Heavy oil
Residue

ABSTRACT

This paper summarizes the technical knowledge necessary to study the hydrocracking of heavy oil with dispersed catalysts. Chemical kinetics aspects of the hydrocracking of heavy oil reaction are reviewed. The discussion also includes a description of the experimental setups, operation modes and suitable reactors for conducting heavy oil hydrocracking experiments. Reactors and their hydrodynamics are described in order to establish the more appropriate operating conditions to perform the experiments. The most common catalyst precursors used in the reaction are listed as well as the analytical techniques employed in characterizing and quantifying gas, liquid and solid samples. Procedures for pretreatment of feed, catalyst dispersion and sulfurization of catalyst precursors are also presented

1. Introduction

Nowadays, the exploration and production of heavy and extra-heavy crude oils, characterized by high content of impurities as well as producing low yields of distillated fractions, has grown as a consequence of the depletion of reserves of light petroleum [1,2]. In this respect the demand for residue and heavy crude oil upgrading by means of hydroprocessing has increased considerably. A simplified diagram for selection of hydroprocessing technologies as function of asphaltenes and metals contents of the feedstock is illustrated in Fig. 1 [3]. Among all the technologies available for hydroprocessing of heavy oil, slurry-phase hydrocracking processes can deal with the highest impurity content of the feed. As a consequence, the hydrocracking of heavy oil with dispersed catalyst has been envisaged as a suitable technology for upgrading heavy petroleum to obtain lower-boiling point valuable products [4]. The reaction of hydrocracking is grouped within the hydrogen addition technologies for upgrading heavy oil. The process is carried out in the presence of a suitable catalyst that provides a double functionality (cracking and hydrogenation). During the process, carbon–carbon bond scissions occur to produce smaller hydrocarbon chains as in thermal cracking but the presence of hydrogen inhibits secondary reactions which ultimately might produce coke. Throughout the text, the term heavy oil is used to refer as a type of crude oil with less than 21° API.

Reactions occurring in slurry reactors offer various advantages over fixed-bed reactors, for example: dispersed catalysts promote faster reactions by lowering the particle size and consequently exposing the entire catalytic surface area to reaction, mass transfer coefficients are higher, the heat transfer in the slurry is also high and highly exothermic reactions can be conducted without the presence of any hot spots, complete wetting of the catalyst is achieved and removal and addition of catalyst can easily be accomplished [5]. In addition, the dispersed catalyst has the ability to prevent excessive cracking and coke formation by releasing activated hydrogen [6].

During the process, catalyst is introduced as fine particles dispersed in the heavy oil. The catalyst consists of dispersed metal sulfides (of iron and/or molybdenum) which are generated by in situ sulfidation of the precursor (generally metallic oxides). As the catalyst is uniformly distributed, the hydrocracking of the high molecular weight hydrocarbons is more efficient [7]. However, hydrodynamics in the reactor, process lines and the equipment must assure that the catalyst is completely suspended, otherwise plugging can occur.

The study of dispersed catalysts performance has been conducted mainly with laboratory reactors with different configuration, e.g. batch, semi-batch, etc. The selection of the experimental setup has been made based on the equipment availability and no much care has been put on a proper choice of it. Other aspects such as type of operation, experimental procedure, separation and

* Corresponding author. Tel.: +52 15523043811.
E-mail addresses: mauricio.angeles@gmail.com, mauricio.angeles@live.co.uk (M.J. Angeles).

0920-5861/$ – see front matter © 2013 Elsevier B.V. All rights reserved.
http://dx.doi.org/10.1016/j.cattod.2013.08.016

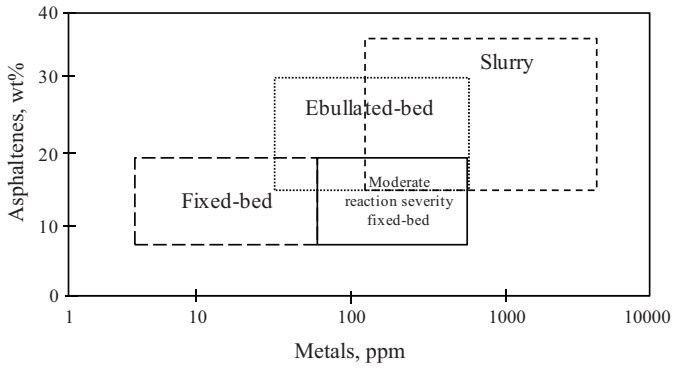

Fig. 1. Typical operating windows for residue hydroprocessing technologies.

analysis of products, have also received less attention when designing the experiments.

It is then the intention of this paper to serve as a guide to design, build or modify an experimental setup and to establish the most suitable experimental conditions to carry out the slurry-phase hydrocracking of heavy oil. For this purpose a description of suitable reactors for slurry-phase process and their hydrodynamics is included. The discussion about the reactors is centered on the appropriate operational conditions that allow the reactor for performing under a kinetic control regime when it is possible. This is done by having an operation where mass transfer limitations are reduced by adjusting the main operational parameters, namely gas and liquid superficial velocity and agitation rate in the case of stirred tanks. The paper also covers the general aspects of the gas–liquid–solid reaction that occur in the hydrocracking of heavy oil together with a state-of-the-art of catalysts, feedstocks and details of the analytical techniques used for characterizing the gas, liquid and solid samples.

2. Preliminary considerations

In multiphase phase reactors, it is common to find that mass transfer and chemical reaction happen as a series of mechanisms. From the microscopic point of view, the complete process is carried out as a series of elementary steps in which physical processes (mass transfer of molecules between phases) and chemical reaction occurs continuously in the reactor. For the case of a three-phase catalytic reaction, these elementary steps are [8]:

1. Absorption of gaseous reactants into the liquid phase.
2. Transfer of reactants to the exterior particle surface.
3. Catalytic reaction.
4. Transfer of products from the exterior particle surface to the liquid phase.
5. Desorption of gaseous products.

The importance of any particular step is defined by the rate at which it occurs and it is related to the concept of the rate controlling mechanism [9]. In a gas–liquid–solid reaction the process is either diffusion or reaction controlled. The controlling mechanism is the process that takes the longest time to occur during the complete reaction process. For this purpose and as analogy with gas–liquid reactions, Astarita [10] and Patterson et al. [11] defined a series of regimes depending on the rate at which the chemical reaction is likely to occur. Mainly, three regimes are met in reaction systems: slow, fast and instantaneous reactions. Nonetheless, transitions between regimes probably take place. This illustrates the complexity of the process and the importance to identify the contribution of any elementary step. From the point of view of chemical kinetics investigation, the ideal conditions during the experimentation are when the reaction time is considerably lower than the diffusion time. Special cases such as those in which the catalysts are completely soluble (indistinguishable in the liquid phase) require particular attention [12].

3. Evaluation of the rate controlling mechanism in gas–liquid–solid systems

The experimental procedure to identify the rate controlling mechanism should include tests that show the effect of catalyst loading, catalyst particle size and agitation in case of stirred tanks or superficial gas velocity for other type of reactors on the hydrocracking of heavy oil reaction [12]. The reaction of heavy oil hydrocracking with dispersed catalysts involves a mechanism of mass transfer between gas–liquid–solid phases coupled with a chemical reaction. Hydrogen is absorbed in the liquid and then it is transported together with the hydrocarbon molecules to the surface of the catalyst particle where the reaction takes place. The oldest and simplest kinetic model of hydrocracking of heavy oil is represented by a power-law of first-order in heavy oil and zero-order in hydrogen concentration [13]. Reaction progression can be followed by changes in the heavy fraction content of the feed.

The steps of the process are defined by [14]:

$$N_1 = k_{GL}a_{GL}(C_{1i} - C_{1L}) \quad \text{(gas–liquid interface)} \tag{1}$$

$$N_1 = k_{LS}a_{LS}m(C_{1L} - C_{1S}) \quad \text{(liquid–solid interface)} \tag{2}$$

$$N_1 = m(-r_{1S}) = mk_C C_{2S} \quad \text{(reaction)} \tag{3}$$

where 1 denotes hydrogen and 2 is assigned to heavy oil. Although the molar flux of hydrogen (N_1) can be represented in terms of diffusion coefficients, it is customarily in engineering to express it as a function of mass transfer coefficients from gas to liquid phases (k_{GL}) and from liquid phase to catalytic particle (k_{LS}) for which there might be already some correlations available. (If equilibrium concentration of hydrogen is used for the equations development, a global coefficient of mass transfer is incorporated into the calculation instead.) C_{1i}, C_{1L} and C_{1S} are the concentrations of the compound 1 at the interface, liquid phase and the surface of the catalytic particle, respectively. a_{GL} is the gas–liquid interfacial area, a_{LS} is the liquid–solid interfacial area, m is the catalyst loading in the slurry and r_{1S} is the reaction rate. Effectiveness factor might be incorporated in the reaction rate in case the reaction is influenced by mass transport inside the catalytic particle pores. For this case, because the catalyst is non-porous it assumed an effectiveness factor of 1.

Since the flux of 1 does not vary along the g–l phases (steady state operation), the flux can be calculated by combining Eqs. (1) and (2) and be expressed it in terms of concentrations at interface and catalyst surface and mass transfer coefficients:

$$\frac{C_{1i} - C_{1S}}{N_1} = \frac{1}{k_{GL}a_{GL}} + \frac{1}{k_{LS}a_{LS}}\left(\frac{1}{m}\right) \tag{4}$$

In the classical treatment of reactions in slurry reactors, only concentrations of hydrogen at the interface or equilibrium are shown in Eq. (4) as a consequence of the kinetics of first-order in hydrogen [15,16]. Here, the term $(C_{1i} - C_{1S})$ is the driving force for the transport of hydrogen. The special case where hydrogen order is zero is not uncommon for hydrogenation reactions and a slightly different approach is followed [17]. One of the first works on the matter was published by Davis et al. [18]. The authors showed that during the fitting of their experiments (which resembles Eq. (4)), the term $(C_{1i} - C_{1S})$ was constant and unaffected by the absorption of the hydrogen in the main body of the liquid. The linearization procedure for reactions of order one is basically the same but the

contribution of the liquid–solid mass transfer and reaction kinetics cannot be separated [19].

Chemical reactions influenced by mass transfer processes are intrinsically more difficult to study because of the series of phenomena involved. Validation of experimental data depends on taking into account appropriately the mechanisms of absorption and chemical reaction separately. For this purpose, it is a common practice in chemical kinetics to establish the rate controlling mechanism [20]. However, this must be confirmed experimentally by assessing the hydrodynamics of the system.

The standard practice for the evaluation of the rate controlling mechanism is carrying out a series of experiments varying the amount of catalyst loading [14,21,22]. By varying the catalyst loading and keeping the rest of the variables constant a plot of $1/m$ versus $1/N_1$ is constructed. The interception of the straight line with the y-axis is an indicative of the influence of the gas–liquid mass transfer in the reaction. If it is considerable (far from origin), a better hydrodynamics in the reactor that allows better contact between gas–liquid phases is required to lower the interception of the line.

Santacesaria et al. [23,24] have demonstrated the application of the method for the hydrogenation step of the synthesis of hydrogen peroxide. Their results showed that zero order reactions exhibited a maximum absorption of hydrogen once the $1/m$ tends to 0. Above this value of m the absorption of hydrogen occurs at lower rate than the chemical reaction. The application of Eq. (4) is only valid before this point is being reached during experimentation. Since it was demonstrated previously by Davis et al. [18] and confirmed by Santacesaria et al. [24] by following two distinct approaches, the term $(C_{1i} - C_{1S})$ remained constant and also $C_{1i} \gg C_{1S}$, thus Eq. (4) can be simplified to:

$$\frac{1}{N_1} = \frac{1}{C_{1i}k_{GL}a_{GL}} + \frac{1}{C_{1i}k_{LS}a_{LS}}\left(\frac{1}{m}\right) \tag{5}$$

And consequently, at infinite amount of catalyst the following approximation holds valid:

$$\frac{1}{N_{1\,max}} \approx \frac{1}{C_{1i}k_{GL}a_{GL}} \tag{6}$$

N_{1max} should be calculated from Eq. (5) considering $1/m \approx 0$. Hence, only C_{1i} is needed to have access to $k_{GL}a_{GL}$. Castañeda et al. [25] have compared the predicted and experimental values of hydrogen absorption for different oil fractions and suggested that correlations proposed by Korsten and Hoffman [26] and Mapiour et al. [27] are suited for the calculation of C_{1i}.

Additional tests are required for the evaluation of the contribution of the liquid–solid mass transfer coefficient. By varying the particle size of the catalyst a plot of $\ln(1/k_{LS}a_{LS})$ as a function of $\ln(d_P)$ is constructed [14]. If the slope of the line constructed is near zero it indicates that the reaction rate is independent of the particle size.

Additional proof can be attained by calculating the activation energy of the reaction. If the value of the activation energy is less than 5 kcal/mol, in the range from 5 to 10 kcal/mol reaction and liquid-absorption might be important. Above a value of 10 kcal/mol the surface reaction might be controlling the reaction.

This method has some limitations, for example when the catalyst particle is smaller than the film thickness of the liquid surrounding the catalyst particles or when the reaction rate is instantaneous and it takes place close to the gas–liquid interface [28].

For the case that catalyst is porous and the intraparticle diffusion is suspected Chaudari and Ramachandran [29] have proposed a method for the analysis of experimental data under a mass transfer influence via the effectiveness factor. In their approach a variation of Eq. (4) was used for the calculation of the concentration inside the catalytic particle.

Once the g–l and l–s resistance have been evaluated it results practical to estimate the interfacial area assuming that both gas bubbles and catalyst particles are considered as spheres:

$$a_{GL} = \frac{6H}{d_B} \tag{7}$$

$$a_{LS} = \frac{6}{\rho_C d_P} \tag{8}$$

where H is the holdup in the liquid, d_B is the gas bubble diameter, m is the catalyst loading and d_P is the diameter of the particle.

Alternatively, Sylvester et al. [30] have proposed a method based on a definition of a generalized effectiveness factor that is used to assess the mass transfer limitations on the chemical reaction rate for slurry reactors. This method is attractive because a vast amount of information can be obtained from only one experiment; however calculations require estimation of values of mass transfer coefficients which are sometimes unavailable for a specific set of chemical species involved in the reaction. If this approach is followed a review of correlations for the calculation of mass transfer coefficients and gas hold-up for three-phase slurry reactor was published by Chaudari and Ramachandran [5] or for the specific case of bubble column reactors the reviews of Shah et al. [31] or Kantarci et al. [32] are available.

As alternative, the evaluation of the gas–liquid mass transfer coefficient can be carried out experimentally by measuring the change in total pressure at the beginning of the reaction [33,34].

The importance of identifying the external factors that might be involved in the reaction will help on the selection of the most suitable laboratory equipment and operating conditions to obtain the most reliable information from the experiments performed.

4. A review of the experimental setups for hydrocracking of heavy oil

Stirred tank reactors operating in batch and semi-batch mode were found to be the most used devices to perform slurry-phase experiments. A summary of the experimental rigs in batch and semi-batch mode for studying the hydrocracking of heavy oil is presented in Table 1. According to this survey there is no published information about the evaluation of mass transfer limitations, internal configuration of the reactor (type of impeller or baffles) or details of operating characteristics such as the minimum impeller speed to assure complete suspension, which is of great importance for choosing the appropriate reactor and its internal configuration. Since the reaction might be affected by mass transfer between phases, these parameters become important if a detailed kinetic analysis of the reaction is performed but also because any mass transfer process might interfere with the catalyst activity interpretation.

Only a few systems were found to operate in a continuous operation mode with different type of reactors. Fathi and Pereira-Almao [35] have studied the hydrocracking of Arab light vacuum residue by steam catalytic cracking using a tubular reactor of 100 ml. Liu et al. [36] performed the hydrocracking of atmospheric residue in a 150 ml reactor. The authors did not provide any specific detail of the reactor design but it might operate as a bubble column or an ebullated bed reactor. Matsumura et al. [37] reported the hydrocracking of a vacuum residue in a continuous stirred tank reactor. Nishijima et al. [38] have investigated a two stage process for upgrading heavy distillates over different catalysts. The authors did not provide any characteristics of the experimental reactor and only operating conditions were mentioned. In all cases the reactor served for catalysts exploration purposes rather than to develop a kinetic model of the reaction. In any case simple setup modifications of the reactor such as incorporation of spargers or in the case of stirred tank

Table 1
Experimental setups for hydrocracking of heavy oil.

Operation mode	Reactor size (ml)	Liquid loading (g)	Catalyst amount (ppm)	Initial H_2 pressure (bar)[a]	Operating temperature (°C)	Reaction time (h)
Batch	30	10	1,000	90	410–460	0.5–0.4
Batch	30	10	0–5,000	80–160	380–460	1.5
Batch	300	30	230–1,400	75	430–460	2.0–10.0
Batch	30	2	200–5,000	90	410–450	0.25–4.0
Batch	50	10.4	15–1,500	93	340	0.5–1.5
Batch	N/A	350	N/A	70	430	2.0
Batch	300	50	435	33	430–460	1.0
Batch	300	100	N/A	103[c]	413	2.0
Batch	100	30	1,000	34.5	320–380	3.0–48.0
Batch	100	30	1,000	34.5	320–380	3.0–70.0
Batch	500	N/A	0–1,000	70	420	1.5
Batch	500	N/A	100–10,000	50	420	1.0–4.0
Batch	165	35	1,000–5,000	N/A	416–436	1.0–1.25
Batch	N/A	N/A	500–5,000	70	435	1.0
Batch	100	40	500–2,500	70	430	1.0
Batch	N/A	143[b]	1,000	41.4 and 55	350–400	1.0–24.0
Semi-Batch	230	50	300,00[d]	80–130 bar and 300 ml/min[e]	430–450	1.5
Batch	50	N/A	N/A	69	310–400	1.0
Batch	300	45	3,000	70	340	30–240
Semi-Batch	250	80	100–1,800	138 bar and 900 ml/min[e]	415–445	1.0
Batch	N/A	N/A	N/A	70	420	1.0
Batch	300	N/A	100–900	55	415	1.0
Semi-batch	250	N/A	100–1,800	138 bar and 900 ml/min[e]	414–445	1.0
Batch	35	10[b]	5,000–20,000[d]	60	330	1.0
Batch	35	10[b]	5,000–20,000[d]	60	330	1.0
Batch	136	10	1,000–10,000	100	410	6.0–12.0
Batch	500	150	100–500	50–80	420–435	1.0
Batch	300	80	360–900	35	400–430	1.0
Batch	1000	380	500	60	420	1.0
Batch	50	3 and 5[b]	N/A	61	350	0.5–3.0
Semi-batch	65	25	1,000	138 bar and 4000 ml/min[e]	380–460	0.15–1.0

Note: Catalyst content is based on the active metal present, N/A: not available.
[a] Initial pressure without heating.
[b] Amount given in ml.
[c] Total pressure at reaction time.
[d] Based on total amount of catalyst.
[e] Specification of the flow rate of hydrogen is also required for semi-batch systems.

reactors a self-inducing stirrer with baffles will be able to improve the reaction performance.

The guidelines provided in the following sections will cover the gap that is usually not included in papers regarding the reactor operation and provide the basis for a more detailed experimental plan and consequently the generation of more reliable information. The considerations go toward producing experimental conditions in which the hydrocracking of the heavy oil reaction is the controlling mechanism. This does not suggest that a proper experimental study to identify mass transfer limitations is not necessary but it is rather a complementary task. In a gas–liquid–solid reaction the evaluation of gradient mass limitations between phases requires an experimental plan to identify the three resistances of the system. The typical experimental test carried out by varying the agitation speed until the conversion is independent is only valid for the case of gas–liquid reactions and it is complementary. For liquid–solid mass transfer limitations only varying the catalyst load in the slurry provide a conclusive test. For the evaluation of the intraparticle mass limitation the particle size should be small enough that conversion of the reaction is not affected by this change.

4.1. Commercial processes for heavy oil hydroprocessing

Since laboratory plants are related to industrial processes, it is appropriate to have a background of the design of processes already in operation. Commercial units devoted to heavy oil hydroprocessing with moving beds are divided depending on the type of operation. Plants are usually operated in ebullated bed or slurry reactors. In the first type of reactors, catalyst is added at the top of the reactor and withdrawn at the bottom, this operation is essential to compensate for catalyst deactivation. Expansion of the bed is controlled by the amount of hydrogen and heavy oil fed to the unit. Once hydrogen and heavy oil reach reaction conditions they are mixed prior the reaction section. After, reaction products are separated and then fractionated. H-Oil and LC-Fining units are perfect examples of the ebullated-bed reactors. The main difference is that meanwhile H-Oil process operates with two ebullated-bed reactors in series, the LC-Fining products from the ebullated bed reactor are fed to a fixed bed reactor [39,40].

On the other hand, slurry technologies can treat heavy oils with a higher content of metals, carbon residue and asphaltenes. Several technologies are available commercially like the Veba Oel's Combi-Cracking, PetroCanada's SRC Uniflex^{TM} (formerly known as CANMET process), Intevep's HDH/HDHPLUS, Asahi's Super Oil Cracking (SOC), EniTechnologie's EST and Headwaters' (HCAT) [4]. The slurry technologies differ from the ebullated bed technologies because the catalyst is added to the heavy oil and then the slurry is mixed with hydrogen before it enters the reactor. Products leaving the reactor are separated before they are fractionated [41].

5. Design of the experimental rig

An important aspect to be considered in the design of the experimental rig is the presence of coke. Coke formation during the hydrocracking of heavy oil is not only a consequence of the ratio of hydrogen to heavy oil. It is indubitable that hydrogen plays an important role during the reaction inhibiting coke formation due to the saturation of the carbonium ions formed during the

Table 2
Comparison of operation in batch, semi-batch and continuous experimental setups.

Factor considered	Type of operation		
	Batch	Semi-batch	Continuous
Amount and cost of equipment	Low	Intermediate	High
Cost of installation	Low	Low	High
Cost of operation	Low	Intermediate	High
Ease of operation	Easy	Easy	Complicated
Amount of reactants required	Low	Intermediate	High
Operational safety	Safer	Safer	Safe
Resemblance with industrial operation	Low	Intermediate	High

thermal cracking process. However, the catalyst is also responsible for avoiding the coke formation and prolonging the coke induction period [42]. Furthermore, operational variables and physical and chemical characteristics of the heavy oils being treated play also an important role [43–45]. Gualda and Kasztelan [46] supported the issue that reversible dehydrogenation reactions responsible for coke formation varies dynamically with pressure, temperature and contact time.

So when the experiment is being planned, it should be addressed the coke formation especially in steady state operation as it was conveniently addressed by Pruden [47] in the hydrocracking of heavy oil for the CANMET slurry process. Coke formation should be taken into account in the design because carbon may accumulate in the reactor or subsequent operations causing plugging [48]. Careful operation planning should be carried out to avoid this problem. On the other hand in batch processes the coke may accumulate in the reaction vessel.

The purpose of this section is to provide the technical information required to establish the basis of design of the experimental rig. Previously, it was described the set of elementary steps involved in the reaction process and how one or some of them can influence the development of the reaction. The following sections will describe the advantages and disadvantages of the operation modes and type of reactors and it should be used as a guide for designing the experimental rig. Bear in mind that at this stage economics aspects of the process are not critical in the decision making process.

5.1. Type of operation

In terms of the type of operation, there are three main modes of operation of experimental rigs. The most simple and common is batch, where reactants are loaded into the reactor at the beginning of the operation and products and unreacted chemicals are collected until the end of the experiment. In hydrogenation reactions, the consumption of hydrogen might cause that total pressure of the system decreases, therefore the ratio of hydrogen to heavy oil decreases over time and only is known at the beginning of the experiment.

On the other hand, if isobaric operation is required, hydrogen can be added through the course of the reaction to maintain the pressure of the system while liquid remains stationary, this type of operation is known as semi-batch. Both batch and semi-batch operations require a minimum amount of reactants and number of additional equipment compared with continuous operation. Something important worth to consider is that in non-continuous operation, the initial reaction time is uncertain. It is commonly accepted that the initial reaction time starts once all reactants are confined in the reactor and operating conditions have been reached. Consequently, it is difficult to assess that prior reaching this point, reactants were unaffected by heating or pressurization of the system. Batch and semi-batch operations are performed in three steps: loading and preparation of reactants (heating and pressurization), reaction and product separation and quantification.

Continuous operation represents a more challenging task in terms of design, construction and operation. Similar to non-continuous mode, the experimental reaction in continuous systems comprises three well defined sections: delivery and preparation of feedstreams, reaction, and product separation and quantification. In the delivery and preparation of the feedstreams section, reactant flow rates are established and operating conditions are met before the streams enter the reactor. The reaction section comprises only the reactor. In the product separation and quantification section, the products leaving the reactor are conditioned for subsequent quantification and analysis. In continuous operation a period of stabilization is needed before the rig reaches continuous operation.

The preferred operation for this particular reaction is batch because it requires the smallest amount of equipment and ease of operation (see Table 1) [49]. On the contrary, continuous operation is more demanding in terms of experimental equipment and operational costs.

Table 2 summarizes the operational characteristics among the three types of processes. Some operational aspects of the hydrocracking process would also support the choice of the batch reactor such as long reaction time and low flow rates of the slurry (which causes fouling in the process due to sedimentation of the solid particles) [50].

5.2. Selection of the reactor

The success of scaling-up any chemical process is based on the reliability of experimental data collected. Being the chemical reactor the center of any chemical process, the reactor selected would impact on the accuracy of the experimental information produced from it. The selection of any type of reactor obeys basically to the nature of the chemical reaction being studied and the aim of the experimental results obtained from it. It is important to identify for example: the number of phases involved, compositions of the streams, complexity of the reaction paths, range of operating conditions, the heat generated or consumed by the reaction, possible reaction products, characteristics of the catalyst (size and shape) or sampling of products among others. The selection of the reactor depends on the available information of mass and energy balances besides the chemical kinetics of any specific reaction. The aim of performing experiments is invariably to provide reliable technical information to discard or continue with the next step of process development.

Table 3 summarizes the three main parameters required for designing a catalytic reactor as suggested by Bartholomew and Hecker [51]. Since the kinetics of the reaction might be not known, the reactor volume cannot be calculated directly, previous experimental information of similar reactions would provide a sensible estimate of the size of the reactor needed for any particular application.

Catalytic hydrocracking reactions can be carried out in a type of reactors denominated slurry because the catalyst is suspended in the liquid phase. Catalyst characteristics in these reactors are

Table 3
Summary of information required for designing catalytic reactors.

Catalyst design	Reactor design	Catalytic reactor design
Mechanical and flow properties	Kinetics of the reaction	Reaction conditions
Catalytic properties	Mass balance	Catalyst type
Physical and chemical properties	Momentum and energy balance	Type of reactor

focused on activity, selectivity and mechanical resistance. These moving bed reactors offer several advantages over traditional operations carried out in catalytic fixed bed reactors, for example [52]:

- The mode of operation can be batch, semi-batch or continuous depending on the needs of the research project.
- Isothermic operation is easier to achieve because liquid has a high heat transfer capacity. The high degree of mixing in these reactors avoids the presence of hot spots in highly exothermic reactions.
- Lowering the size of the catalytic particle allows better transport of molecules between liquid and solid phases limiting diffusion limitations.
- Ease of catalyst addition or removal.

However its operation has some drawbacks like:

- Abrasion in the pipelines due to the presence of solids.
- Catalyst attrition causes accumulation of fine particles in the reactor.
- The complexity of the reactor hydrodynamics makes it difficult to scale-up.

Weekman [53] reviewed a series of experimental reactors and provided a comparison among them based on five operational categories. Due to the type of reaction only those reactors that can cope up with slurry phase reactions were considered. Table 4 shows the results of the comparison among the experimental reactors. At laboratory level, three types of reactors were chosen as the best alternatives. These reactors are the mechanically agitated tank slurry reactor which is extremely flexible as it can be operated in batch, semi-batch or continuous mode, the bubble column slurry and the three-phase fluidized-bed reactor that fall into the straight-through and recirculating transport reactor categories. The distinction between bubble column and three phase fluidized bed reactor is the mechanism that is employed to transfer momentum within the reactor. In the former the momentum is transferred by sparging the gas into the liquid meanwhile in the latter the momentum is transferred by the liquid movement. The mode of operation is flexible in the bubble column reactor because the liquid phase could be in steady state whereas the gas is sparged into the liquid or both phases are fed in continuous in cocurrent or countercurrent mode. The three-phase fluidized bed is limited in this way because the liquid provides the momentum transfer and only operation in continuous mode is possible. The fluidized bed operation is carried out in cocurrent and countercurrent. The advantage of the fluidized bed reactor is that it can handle larger particle sizes and thus catalyst separation is easier than in the other two types of reactors.

5.2.1. Experimental considerations for the operation of the laboratory reactor

It should be pointed out that if the main purpose of the reactor is to develop kinetic studies of reactions only chemical reactors with flow pattern close to ideal models should be considered. Any real chemical reactor finds its operational boundaries in the performance of the continuous stirred tank (maximum mixedness) and the plug flow reactor (completely segregated) [54]. For this reason, it is important to consider that if chemical kinetics studies will be performed, the stirred tank reactor operating in batch, semi-batch and continuous mode should be first considered. The main disadvantage of the bubble column and fluidized bed reactor in chemical kinetics is their poor performance due to the poor backmixing. These reactors should operate with a high ratio of recirculation to resemble the conditions of maximum mixedness characteristic of stirred tank reactors. If operation close to an ideal reactor can be achieved the kinetics of the reaction can be obtained from a relatively simple mathematical expression. For catalyst exploration and evaluation there is not restriction on the type of reactor but the results should be cautiously interpreted.

It is difficult to point out an ideal experimental reactor because its selection will depend on many factors. Basically, stirred tank reactor offers the highest flexibility among other reactors because they can be operated in batch or semi-batch without any major changes in the experimental setup or in a continuous mode. These type of reactors are perfect for kinetic studies provided that deviations from ideal behavior are minimal (gradientless in temperature and concentration).

If premixing of the streams before entering the reactor is envisioned in the experimental plant design, static mixers should be considered for the operation [55]. Mixing devices can be chosen for the operation depending on the flow regime (laminar, transition or turbulent) of the streams but static mixers are suitable for gas–liquid mixing independently of the flow regime. Static mixers improve considerably the axial mixing of both phases and because of this they can even be used as a double-purpose devices (mixing and reaction) [56,57]. If mixing of the streams is not accomplished in a static mixer, it is usually a good practice to allow a minimum distance of 100 times the internal diameter of the tubing before entering to the following stage in the process [16].

Sampling is critical in kinetic studies and perhaps a difficult operation to accomplish in any type of process. If it is carried out in a non-steady reactor the volume of the sample should not affect the total volume of the reactor. Sampling should be carried out in a system that allows a fast cooling and efficient storage to avoid any misinterpretation of the data.

Another possible operational problem encountered in hydrocracking of heavy oil is the possibility of plugging in the equipment

Table 4
Comparison of experimental reactors [53].

Reactor characteristics	Stirred batch	Continuous stirred tank	Straight-through transport	Recirculating transport
Sampling and analysis	F	F	F-G	F-G
Isothermality	G	G	P-F	G
Residence and contact time	G	F-G	F-G	G
Selectivity disguise-decay	G	G	G	G
Construction problems	G	P-F	F-G	P-F

Note: G = good; F = fair; P = poor.

[48]. Cracking of long hydrocarbon chains produces inevitably coke and sludge which can reduce the operation efficiency.

Mixing is the main factor that overcomes the mass transfer resistance in the reactor but only affects the gas–liquid resistance and consequently other factors might be varied [58]. In order to lower the liquid–solid resistance, utilizing small catalyst particles with high superficial area should avoid this drawback. To avoid the pore diffusion it is recommendable to use very small particles. In an experimental plan, it is useful varying some of the reaction parameters (agitation speed, catalyst loading, catalyst size, hydrogen concentration or reactants flow rate or total pressure of the system) between experiments to identify any major contribution of the operational parameters.

5.2.2. Mechanically stirred tank reactor

As it was stated previously, the stirred tank reactors are without any doubt the most common chemical reactor found in a laboratory. The reactor can be easily adapted to accomplish the purpose of any specific reaction (kinetic studies and catalysts tests) [59]. Mechanically stirred tanks are generally used for the purpose of studying heavy oil hydrocracking reactions [49]. There are many factors to consider for the selection of the reactor and the literature is extremely rich regarding stirred tanks. For this reason, the information presented here was narrowed to the ideal configuration to study a three-phase reaction.

In a reactor of this type, the main parameter to be considered is the agitation. Mixing should accomplish the following:

- Create a high interfacial area that promotes mass transfer between the gas and liquid phases.
- Maintain in suspension and homogenized the solid particles in the liquid phase.
- Increase the heat transfer between the solid and liquid phases.

The parameters considered here are related mainly with the hydrodynamics of the reactor. Stirring systems promote faster transfer of mass from gas to liquid phases; this gas absorption rate is proportional to the interfacial area created between the phases in the reactor. Consequently, mainly the speed of agitation and the type of impeller are fundamental for the creation of the gas liquid interface. In a gas–liquid operation the interface area is primarily conformed by the bubbles created by the dispersion of the gas in the liquid rather than only the area between the gas head space and the liquid. For practical purposes, this area is negligible with respect to the interface area created during the mixing of the reactor [60]. Thus, rate of bubble formation, size, breakup and coalescence play a major role in the prediction of gas–liquid transfer coefficients.

The selection of the complete configuration of the agitation system for the reactor includes: stirrer type, gas sparger, wall baffles and speed of agitation. Sizing and positioning the agitation system play also an important role in the efficiency of mixing in the reactor. Mixing in a multiphase system dictates the performance of the chemical reaction. Under turbulent flow, gas–liquid mass transfer coefficients are controlled by the gas fraction in the system and the power dissipated by the stirring system. Mixing is a very complex process that takes place at three different levels in the system. Macromixing is carried out at reactor level and it is a global process that involves mesomixing and micromixing. Meanwhile, micromixing occurs at molecular level and it is responsible for changes in the product quality. Mesomixing takes place at intermediate scale and it is present for example when fresh feed interacts with its surroundings [61]. A rigorous mathematical model of the reactor should be able to account for all three process of mixing.

Most of laboratory stirred tank reactors are supplied with mechanically agitated stirrers (a less common case is the shaking autoclave [62]). It is advisable to have a variable speed motor which

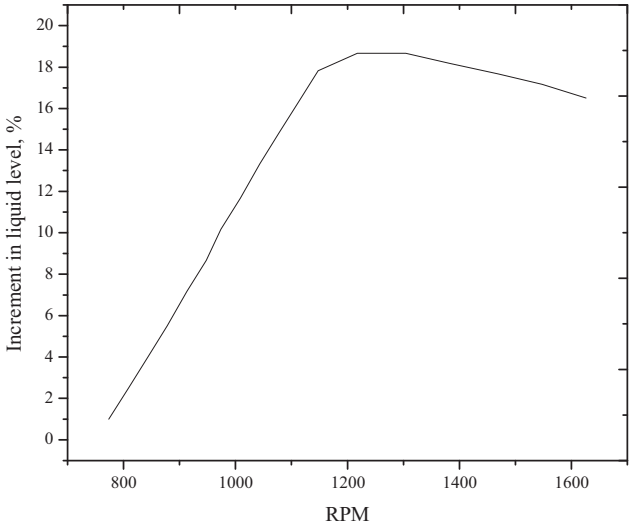

Fig. 2. Change in liquid level by effect of the agitation speed (courtesy of Parr Instrument Company).

can be used to study the effect of stirring speed on the chemical reaction. Consider that there is a change in volume of liquid by effect of the increment in the agitation speed as it shown in Fig. 2. The study was performed in a 600 ml vessel using air and water. The results might be different if the system changes but this value should be considered as an approximation.

Perhaps the key step in the stirring system is the selection of the type of impeller. The choice of a specific type is made respect to the type of application and with respect to the viscosity of the liquid. In gas–liquid–solid systems, the impeller should keep the solids in suspension, maintain a homogeneous concentration of the slurry and reach a high degree of gas–liquid dispersion. Blade turbines and propellers are used for liquids with low viscosity usually between 0.001 and 40 Pa s. Liquids with higher viscosities require wide-radius or screw-type stirrers.

The best type of impellers for gas–liquid mixing is a type of turbine known as self-inducing, gas entrainment or hollow stirrer [63]. Self-inducing impellers have a hollow shaft with a gas entrance at the top part of the stirrer and openings at the blade tips (Fig. 3). Gas from the head space is circulated to the tip of the turbine due to a difference in pressure between the top part of the shaft and the tip of the blades which is created by the agitation of the stirrer. This pressure difference is sufficient to overcome the static column of liquid and gas simply circulates inside the hollow shaft [64]. The performance of the hollow stirrers is favored at high rotor speed and with the use of baffles. Mass transfer coefficients increases considerably with a self-inducing stirrer over a standard impeller [59]. However, self-inducing impellers do not guarantee that the solid distribution in the reactor is uniform. Impellers should operate in a flow regime of complete dispersion that is reached when gas bubbles are circulated efficiently in the vessel and avoid other operation regions where mixing is poor due to localized dispersion for example at the top part of the vessel (loading) or when the gas only flows around the shaft of the impeller (flooding) [65].

Impellers are also designed depending on the type of mixing operation required. Typically, impellers are divided according to the type of flow that generates in the vessel. Axial flow impellers generate a flow pattern that is extended above and below of the stirrer and this creates a sweeping action that maintains solid particles in suspension. Meanwhile, radial flow impellers establish a liquid flow pattern toward the wall of the vessel and they are mainly used for gas dispersion. When are located close to the bottom of the vessel axial flow impellers produce a radial flow in the bottom of

Fig. 3. Self-inducer stirrer (courtesy of Parr Instrument Company).

the vessel. Radial flow impellers can suspend solid particles if they are located close to the bottom of the vessel but in this respect are less efficient than axial impellers. The impeller influences the mass transfer processes in the reactor since it affects the hydrodynamics of the reactor (gas dispersion in the liquid phase).

There is a series of guidelines in literature that can be followed to improve the mass transfer in stirred tank reactors. For example, if the ratio of liquid height (Z) to tank diameter (D_R) is higher than 1 more than one impeller might be required (Fig. 4). As a rule

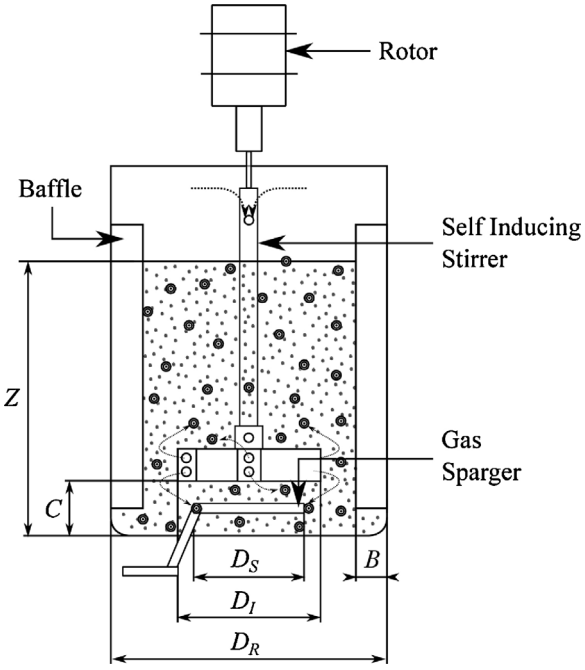

Fig. 4. Mechanically stirred tank reactor.

Table 5
Design parameters for a stirred tank reactor.

Design parameter	Specification
Impeller diameter, D_I	$0.35D_R - 0.5D_R$
Space between multiple impellers	D_I
Reactor bottom clearance, C	$D_R/4 - D_R/6$
Wall baffle, B	$D_R/10 - D_R/12$
Wall baffle clearance	$0.015D_R$
Sparger diameter, D_S	$0.75D_I - 0.8D_I$

dual impellers are needed when $1.3 < Z/D_R < 2.5$ [66]. In this case, the distance between impellers should be at least the impeller diameter (D_I). The ratio of impeller diameter to vessel diameter (D_I/D_R) should be for a flat bottom vessel $D_I/D_R = 0.45 - 0.5$, for a dished bottom vessel $D_I/D_R = 0.4$ and for a spherical bottom vessel $D_I/D_R = 0.35$ [67]. The space between the tank bottom and the impeller or clearance (C) should be between $D_R/4$ and $D_R/6$. The first value is recommended for solid suspension while the last value is suggested for optimal gas dispersion.

The use of baffles is also necessary to avoid any vortex around the impeller shaft and to distribute appropriately the gas and catalyst. Wall baffles are installed for transitional and turbulent mixing and low viscosity fluids. The swirls motion in the liquid produced by the impeller is transformed into top-down or axial flow that allow lifting and maintaining the solids in suspension. Wall baffles (B) are usually dimensioned in relation to the tank diameter that is usually in the range of $D_R/10$ to $D_R/12$. To minimize dead zones between the baffle and the tank wall a space of at least 1.5% of D_R is advisable [68]. Four baffles is usually the most common configuration in stirred vessels.

A gas sparger also promotes better mixing between gas and liquid phases and to allow a better distribution of the gas in the vessel. It is preferable to have a ring sparger rather than a single nozzle to disperse the gas. The sparger diameter (D_S) is dimensioned in relation to the impeller diameter, it is suggested to have a ring sparger of $1.5D_I < D_S < 2D_I$ [69]. Nevertheless, other authors suggest that the sparger diameter should be $0.75D_I$ to $0.8D_I$ [67,68]. Internal space will dictate the size of the ring sparger and it should be located as close as possible to the impeller.

Table 5 summarizes the internal specification of the mechanically stirred tank. The parameters presented here represent a collection of the most common parameters found in specialized literature. Modification of any existing reactor to satisfy most of the design requirements to cope up with gas–liquid–solid reactions should be made under manufacturer approval.

5.2.2.1. Catalyst suspension. The presence of the particles in the system creates different hydrodynamics that in a gas–liquid system. Consequently, correlations taken from gas–liquid systems do not hold completely valid for gas–liquid–solid systems. An example is the correlation proposed by Zwietering and later modified by Baldi et al. [70–72] for the calculation of the minimum agitation speed for complete suspension:

$$N_{\min} = \frac{\beta \mu_L^{0.17} (\rho_P - \rho_L)^{0.42} g^{0.42} d_P^{0.14} m_1^{0.125}}{\rho_L^{0.58} D_I^{0.89}} \quad (9)$$

where μ_L is the liquid viscosity, ρ_P is particle density, ρ_L is the liquid density, g is the acceleration due to gravity and m_1 is the catalyst loading in g/100 g of solution. β can be calculated from:

$$\beta = 2\left(\frac{D_R}{D_I}\right)^{1.33} \quad (10)$$

If agitation is not enough to keep the slurry in suspension, the solids might precipitate. Even though this expression underpredicts the value of the minimum agitation speed for complete

suspension when gas is introduced into the system, it can be taken as a sensible estimate. Accordingly, a more suitable correlation is needed for three-phase reactors like the one proposed by Rewatkar et al. [72] and Rewatkar and Joshi [73]:

$$N_{\min} = 5.56 \frac{\left(V_{SP}^{0.5} - 0.9V_{SP}^{1.27}V_C\right)}{D_I^2} D_R m_1^{0.1} V_{SG}^{0.14} \quad (11)$$

where V_C is the liquid circulation velocity, which is calculated from:

$$V_C = 0.196 N D_I D_R^{-0.11} V_{SG}^{-0.262} \quad (12)$$

N is given in revolution/s and V_{SG} is the gas superficial velocity in m/s. The V_{SP} is the particle settling velocity which is calculated as a function of the Reynolds number using V_{SP} [67]:

$$Re_{SP} = \frac{V_{SP}\rho_L d_P}{\mu_L} \quad (13)$$

According to the Reynolds number, the V_{SP} is calculated from:

- Stoke's regime

$$V_{SP} = \frac{g d_P^2 (\rho_P - \rho_L)}{18\mu_L} \quad Re_{SP} < 0.4 \quad (14)$$

- Intermediate regime

$$V_{SP} = \left[0.0178 \frac{g^2(\rho_P - \rho_L)^2}{\rho_L \mu_L}\right]^{1/3} d_P \quad 0.4 < Re_{SP} < 500 \quad (15)$$

- Newton's regime

$$V_{SP} = \left[3.1 d_P \frac{g d_P (\rho_P - \rho_L)^2}{\rho_L}\right]^{1/2} \quad 500 < Re_{SP} < 2 \times 10^5 \quad (16)$$

In a stirred tank reactor the liquid phase should be completely backmixed, this condition is fulfilled in a turbulent regime of operation. The turbulent regime is reached when the Reynolds number of impeller (Eq. (17)) is 10,000 or higher. This condition assures a state of complete mixedness in the liquid phase.

$$Re_I = \frac{N D_I^2 \rho_L}{\mu_L} \quad (17)$$

where N is the speed of agitation. Although commonly gas–liquid data can be applied in some cases, the addition of the catalyst causes changes in the gas–liquid adsorption data. Data extrapolated from the gas–liquid systems should be used cautiously.

The main limitation of the use of a stirred tank reactor in batch or in continuous operation is during the scaling-up operation. Deviations from ideal reactor behavior have implications in conversion and selectivity. Assumption of an ideal reactor is a common practice but it is not easy to achieve at laboratory scale. This reactor is also called gradientless since mass and temperature are uniform in the vessel. This is critical especially for fast reaction rates that can cause concentration and heat gradients in the system [74]. The guidelines suggested in this section aim to assure that deviations from ideality are minimal, if reactor configuration and operational conditions are met during experimentation.

For the case of self-inducing impellers the correlation proposed by Zieverink et al. [75] can be applied to calculate the critical speed for the onset of gas induction:

$$Sh = 10^{-3.35} Re^{1.50} (Fr - Fr_C)^{1.12} Sc^{0.81} \quad (18)$$

Here the Sherwood number is defined as $Sh = k_{GL}a_{GL}D_I^2/DA$, Reynolds number (Eq. (17)), Froude number $Fr = N^2 D_I{}^2/(gZ)$, critical Froude number $Fr_C = N_{crit}^2 D_I{}^2/(gZ)$ where N_{crit} is the critical agitation speed, Schmidt number $Sc = \mu_L/D_A\rho_L$. In the previous equations, $k_{GL}a_{GL}$ is the volumetric mass transfer coefficient and D_A is the hydrogen molecular diffusivity.

When reactor configuration includes self-inducing impellers the correlation proposed by Hichri et al. [76] can be used to calculate the mass transfer coefficient.

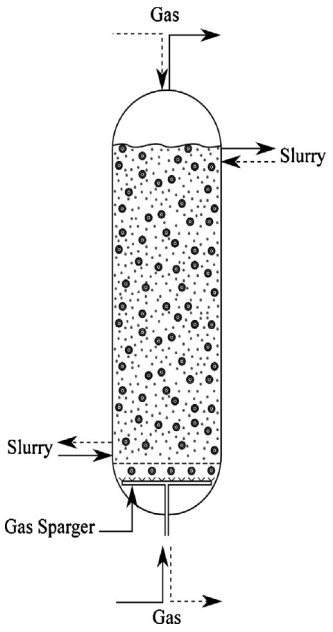

Fig. 5. Bubble column reactor.

5.2.3. Bubble column reactor

In industry, bubble column reactors are the most common type of slurry reactors. Bubble column reactors have the advantage of a large heat and mass transfer coefficients and easy removal or addition of catalyst. Moreover, they provide higher interfacial surface area (approximately 30%) and consequently larger mass transfer coefficients than stirred tanks [77]. Bubble column reactors are multiphase systems in which the gas feedstream is continuously bubbled into a liquid phase (Fig. 5). The vessel generally is an empty tube placed vertically but there are different configurations with internal devices to promote the mass transfer such as sieve trays, packing material or static mixers [78]. In industry the reactor is dimensioned with a length to diameter ratio of at least 5. Large ratios promote higher conversions and high pressure drop but also low ratios favor a higher gas throughputs and it becomes an optimization problem to find the suitable size of the reactor. The momentum transferred by the gas bubbles produces a mixing in the vessel that promotes mass transfer between phases. Operation in bubble column reactors is flexible respect to the contacting mode between gas and liquid; in the simplest type the liquid phase is stationary while gas is sparged through the vessel. When both streams are operated continuously, the contact between phases occur cocurrent (upflow or downflow) or countercurrent. Higher mass transfer coefficients are obtained in downflow systems because of the longer residence time of the gas in the vessel.

For modeling purposes, the gas stream is considered to move in plug flow or complete backmixed along the reactor whereas the liquid phase is considered to be completely backmixed. The assumption of complete mixedness in the liquid is not completely valid especially if high conversions are obtained. This can be overcome by the introduction of a liquid recirculation loop to reach a complete backmixed regime. In this way the material balance is obtained from relatively simple algebraic equations [79]. Without

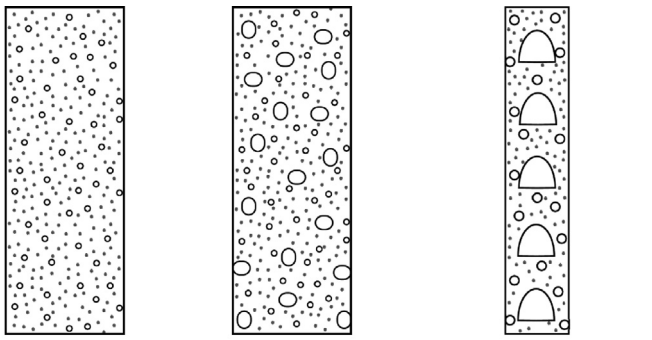

Fig. 6. Schematic representation of the flow regimes in bubble column reactors.

the loop, the reactor might perform poorly which is an enormous disadvantage for studying chemical kinetics since the mathematical expression of the reactor model can become complex. The axial dispersion model is often used for mathematical modeling of bubble column reactors but Dudukovic et al. [80] stresses the fact that there is still lack of a reliable model to predict the reactor performance due to the complex interactions of the fluid dynamics and the appropriate model for the coefficient of mass transfer. In slurry reactors, there is an extremely complex link between operational conditions and bubble behavior, gas holdup and liquid velocity which greatly defines the hydrodynamics and performance of the reactor [81]. While other variables also have some sort of influence in the process performance, the gas velocity defines to a great extent the behavior of the reactor.

Modeling of bubble column reactor has been successfully performed for the case of heavy oil hydrocracking. The hydrodynamics of the reactor has been coupled with the kinetics of the hydrocracking of heavy oil reaction allowing a suitable representation of the reaction products distribution [82–84]. Two dimensional models were used to represent the complexity of the hydrodynamics of the bubble column reactor, however, there are still some limitations of the model regarding the dispersion and mass transfer limitations. However, the flow pattern in the bubble column reactors did not affect considerably the conversion [85].

5.2.3.1. Reactors flow regimes. In bubble column reactors mainly three types of flow can be identified [86] (Fig. 6). The homogeneous regime is defined for a uniform bubble size and bubble distribution in the axial and radial direction of the vessel. When gas flow rate is increased considerably, the heterogeneous regime is developed. This regime is characterized by the presence of a wide distribution of bubble sizes which agglomerate due to the high speed of the gas stream. The last regime found especially in small diameter reactor at high gas flow rates is the churn turbulent or slug flow. In this regime the coalescence forms gas bubbles which size is compared to the reactor diameter. As they move through the reactor, there is an intermittent outlet stream of gas and liquid (dilute and dense zones). The transitional regime lies in-between the regimes. Establishing boundaries between regimes is rather difficult because they depend on many characteristics of the system such as liquid viscosity, gas flow rate, loading of catalyst, pressure, etc. The type of regime in a bubble column reactor affects directly the conversion and selectivity of the reaction.

To establish adequate operational conditions to carry out experiments in bubble column reactors, an equation to calculate the maximum allowable superficial gas velocity was derived from published data [32]. This equation allows for calculating the maximum gas velocity to maintain a homogeneous bubble flow in the reactor:

$$V_{SG\,max} = 5.1322 + \frac{-7.0311}{[1 + (D_R/1.2625)^{1.2036}]} \times 2.5\,cm \le D_R \le 100\,cm \quad (19)$$

where V_{SGmax} is given in cm/s and D_R must be in cm. Once the superficial gas velocity is calculated from Eq. (19), this value is the maximum allowable to assure that the reactor will perform in a homogeneous regime. Since in bubble column reactors the momentum transfer depends solely on the gas flow rate, the reactor diameter is only required to calculate the maximum gas velocity. Values close to the V_{SGmax} should be avoided since the boundary between different types of flow is not defined with accuracy.

5.2.3.2. Sparger design. The gas introduction into the column dictates the hydrodynamic behavior of the reactor. Gas holdup and consequently mass transfer coefficients depend greatly on the way that gas is dispersed into the liquid. For the most common configuration of the bubble column reactor, the gas is fed at the bottom of the column by a gas sparger. The gas sparger must distribute homogeneously the gas supplied to the reactor and it should create a uniform bubble size distribution that allows for developing a homogeneous flow regime in the column. There are several designs of spargers that go from simple perforated pipes or plates to porous discs. The use of any gas sparger will be in function of the type of reaction that is carried out but generally porous discs should be avoided because of the high pressure drop and their tendency to be clogged due to the small catalytic particles. In the case of pipe gas distributors, these are made in the form of rings, spiders or radial spargers. Maldistribution of gas can be avoided by varying the pipe diameter and free area along the pipe (changing diameter of the holes or the free space between them) and feeding both ends of the sparger [87]. The design of the sparger is complex since involves a series of operational, process and manufacturing considerations. Kulkarni and Joshi [88,89] have suggested based on a comparison of different gas spargers that wheel spargers are the best gas dispersion devices for bubble columns. The comparison was made over a considerable range of operating conditions and different reactor design parameters.

A critical point is to design an efficient sparger that allows an even flow from each orifice. To assure an even flow from each perforated point in the sparger some criteria must be fulfilled [90]:

$$\frac{KE_{in}}{\Delta p_0} \le 0.1 \quad (20)$$

where KE_{in} is the kinetic energy of the gas at the inlet of the pipe,

$$KE_{in} = \frac{\alpha V_{G\,in}^2}{2g} \quad (21)$$

V_{Gin} is the gas inlet velocity and $\alpha = 1.05$ for turbulent flow and $\alpha = 2$ for laminar flow. Other criteria can be drawn in terms of gas velocity at the orifice ($V_0 \le 76.2 - 91.44$ m/s), its Reynolds number ($Re_0 \ge 6000$) or based on the Weber number but data of interfacial tension of the gas is needed [86].

5.2.3.3. Catalyst suspension. The last operational parameter of a bubble column reactor is the minimum superficial gas velocity to reach complete suspension of the particles. The minimum superficial velocity for total suspension can be calculated from the following mathematical expression [16]:

$$V_{SG\,min} = \gamma_1 \left(\frac{D_R}{2}\right)^n V_f \exp(-\gamma_2 \varepsilon_P) \quad (22)$$

where ε_P is the volumetric fraction of the reactor occupied by the solid and the coefficients are determined according to the value of

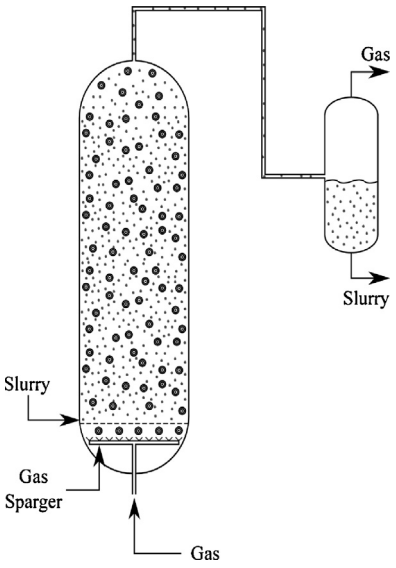

Fig. 7. Three phase fluidized bed reactor.

ε_P. If $\varepsilon_P < 0.1$ then $\gamma_1 = 4.3$ and $\gamma_2 = 10$ or when $\varepsilon_P > 0.1$ then $\gamma_1 = 1.25$ and $\gamma_2 = 3$. The value of n is determined by the size of the particles. When particles are about 100 μm or smaller $n = 0.2$ or in the case that particles are bigger than 200 μm the value of n is 0.5.

The value of V_f is determined from the following equation:

$$V_f + 3.687 H_S^{0.5} (V_f)^{\gamma_3} = \left[2g(\rho_P - \rho_L) \left[\frac{2d_P}{3\rho_L} + \frac{\varepsilon_P H_S}{\rho_P + \varepsilon_P \rho_L} \right] \right]^{0.5} \quad (23)$$

$\gamma_3 = 0.5$ when V_f is lower than 6.7 cm/s. In case that V_f is in the range of 6.7–21.3 cm/s the value of γ_3 is 0.19. This equation is very useful because only requires values that are already available. If a comparison is required some other correlations for the minimum superficial velocity were proposed by Koide et al. [78,86], Roy et al. [91] or Immich and Onken [92].

5.2.4. Three phase fluidized bed reactor

Three-phase fluidized bed or ebullated bed reactors are commonly used for the upgrading of heavy crude oils and for this reason there is an increasing interest in studying in detail the link that exits between the hydrodynamics of the reactor, the mass and heat transfer and their effect on the kinetics of the reaction [93]. In a three phase fluidized bed reactor, gas and slurry are usually fed in cocurrent manner with both streams moving upward along the reactor (Fig. 7). Larger catalyst particle sizes in comparison with other slurry reactors can be handled by the system since liquid is mainly responsible for the momentum transfer in the reactor. Hence, the continuous operation of ebullated bed reactors is more attractive because catalyst separation is easier to achieve. Nevertheless, the catalyst is preferably kept in the reactor by adjusting the liquid flow rate and consequently the bed expansion. To assure that the catalytic particles are maintained in suspension at all times it is important to identify the minimum liquid velocity required for this condition in the reactor. Although, the use of some mathematical expressions from two phase systems can be extrapolated to a gas–liquid–solid systems, in ebullated bed reactors the interactions of the solid particles with the other two phases is stronger and a different hydrodynamics is developed in the reactor.

5.2.4.1. Reactor flow regimes. In a fluidized bed the liquid velocity is mainly responsible for the type of flow that is developed in the column at low gas velocities. The classification of flow patterns in ebullated bed is wide and complex and consequently at least seven flow patterns were identified [94]. Experimental data used to produce the map of the flow rates cannot be accurately extrapolated to a different set of three-phase systems. As an attempt, to simplify the classification of flow patterns encountered in fluidized bed and to identify the boundary of the most suitable operational conditions to perform the experiments, the flow regimes were reduced to three flow regimes [67,86]. The classification according to superficial velocities shows the bubble-flow, slug-flow and gas continuous regime. In the bubble-flow pattern gas bubbles and slurry are homogeneous in the reactor. Gas bubbles are uniform and move faster than the liquid. When gas superficial velocity is increased, gas tends to form big slugs and it produces a clear division between portions of fluid of low and large density. In the slug-flow regime, low and large density fluid portions abandon the reactor periodically and not as a single phase as in the bubble-flow regime. When gas superficial velocity is comparatively high with respect to liquid superficial velocity, the reactor is converted to a gas continuous system and liquid becomes dispersed in the gas. The information on the boundaries between the systems is not completely precise and it is often taken from visual inspection.

In parallel three other flow regimes are encountered when the distinction is based on the type of fluidization. These patterns are particulate fluidization, aggregative fluidization and transition state fluidization. There is a correspondence between the two types of classifications. In particulate fluidization, the solid is distributed evenly in the reactor which resembles the bubble-flow regime. Meanwhile, aggregative fluidization is characteristic of large gas superficial velocity as when gas is the continuous phase in the reactor. The transition between these two phases is known as aggregative fluidization and is usually encountered in the slug-flow regime. Due to the great interest in ebullated bed reactors there has been considerable research advances in this area. Duduković et al. [80] showed this boost of available information (empirical and phenomenological) for three phase fluidized bed reactors. The authors indicated a wider flow pattern classification based on novel characterization techniques. This effort is not overlooked but for the purpose of this paper, the information presented in the subsequent parts of this section will be narrowed to operating conditions that simplify the experimentation.

When a fluidized bed is in operation, it is usually preferred to have a homogeneous system as represented by the bubble flow or particulate fluidization. Although, both regimes practically overlap over the same operational region of the reactor there is a subtle difference among their boundaries.

To assure that the flow inside the vessel is in fluidized regime two equations were derived from published data [16]. Once a certain superficial liquid velocity has been established for the reactor, the minimum superficial gas velocity to operate in fluidized bed regime is calculated from Eqs. (24) and (25). The minimum superficial velocity is given at standard conditions of pressure and temperature and in m/s. Above this value, it is guaranteed that the reactor operates in homogeneous regime.

$$V_{SG\,min} = 0.018 + 0.3182 \exp\left(-\frac{V_{SL}}{0.0015}\right) \times 0.002\ \text{m/s} \le V_{SL} \le 0.005\ \text{m/s} \quad (24)$$

$$V_{SG\,min} = -1.5817 + 1.6389 \exp\left(-\frac{V_{SL}}{0.2913}\right) \times 0.005\ \text{m/s} \le V_{SL} \le 0.01\ \text{m/s} \quad (25)$$

where V_{SL} is the liquid superficial velocity.

5.2.4.2. Catalyst suspension. As in the previous two types of slurry reactors it is important that the catalyst is maintained in total suspension. The total suspension assures that all the catalyst active

area is wetted and consequently available for the reaction. The following equation proposes the minimum liquid superficial velocity necessary for the complete suspension of solids [16]:

$$V_{SL\,min} = 5.121 \times 10^{-3} \left(\frac{\mu_L}{d_P \rho_L}\right) Ar_L^{0.662} Fr_G^{-0.118} \quad (26)$$

where Ar_L and Fr_G are the Archimedes and Froude numbers for liquid and gas, respectively. These dimensionless numbers are defined as follows:

$$Ar_L = \frac{\rho_L d_P^3 (\rho_P - \rho_L) g}{\mu_L^2} \quad (27)$$

$$Fr_G = \frac{V_{SG}^2}{g d_P} \quad (28)$$

Eq. (26) is not applicable at low gas superficial velocity. The correlation presented here is rather simple and only depends on physicochemical properties of the system already available. However, there are in literature some other mathematical expressions that are produced by analyzing the phenomenon of three-phase fluidized reactor [80]. Perhaps, the definitive word on the calculation of the V_{SLmin} was proposed by Larachi et al. [95]. The correlation produced by the authors is based on a thorough analysis using neural networks of a wide set of data of different gases, liquids and bed properties.

A key aspect in the design of a fluidized bed with three phases is to have an efficient device to disperse and distribute the gas uniformly in the column. Design of sparger can be carried out following the guidelines from the previous section. Although high pressure and temperature decreases gas bubble size in the column, this operating condition does not guarantee homogeneous gas distribution.

5.3. Considerations for the experimental rig configuration

There are not standard guidelines for designing experimental rigs as it usually occurs at industrial scale. At laboratory reactor level, the design relies more on previous experience with similar process or by adapting an already installed experimental setup to cope up with the new process needs. The experimental rig is divided in three main stages (non-steady operation) or sections (steady operation): the delivery and preparation, reaction and separation, cooling, depressurization and sampling. Once the reactor and mode of operation have been defined, the next stage is to calculate the mass and energy balance of the complete operation. After the laboratory rig is being configured, it is advisable to carry out a simulation of the experimental plant in a process software simulator to identify any additional need of process equipment (such as phase separators, heat exchanger, etc.) and to identify any probable cause of error in the rig mass balance (i.e. loss of light hydrocarbons in certain parts of the rig) in certain sections of the plant. The rest of equipment will be selected according to the mode of operation of the experimental setup.

5.3.1. Configuration of the experimental rig for batch and semi-batch operation modes

These two modes of operation result in the lowest investment in laboratory equipment. Stirred tank reactors are usually chosen as laboratory reactors for this type of operation. Fig. 8 shows a simple process diagram of the experimental rig. In the diagram the hydrogen is supplied by gas cylinders connected directly to the reactor. The total mass balance is carried out by measuring accurately the initial amount or flow of hydrogen and hydrocarbon and liquid and gas product streams. Liquid product quantification might be made by weighting before storage for subsequent analysis while gas quantification requires a flow meter for total gas quantification and

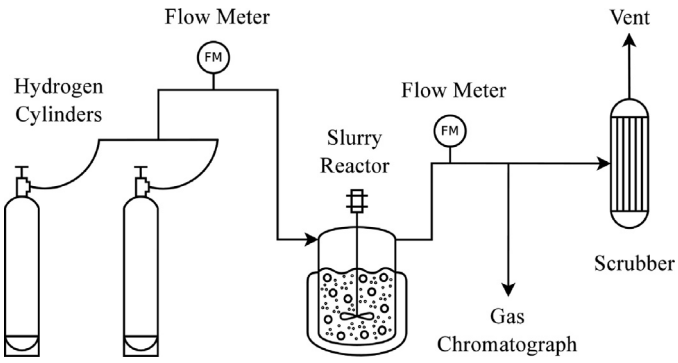

Fig. 8. Diagram of the experimental rig for hydrocracking of heavy oil in batch and semi-batch operation modes.

online analysis by gas chromatograph. Gas product stream contains mainly unreacted hydrogen and a mixture of reaction products which comprises light hydrocarbons, hydrogen sulfide and carbon and nitrogen oxides. A scrubber is located before venting the gases to remove mainly hydrogen sulfide from the stream.

In the case of semi-batch operation hydrogen is added continuously from the cylinders. In batch mode the decay of pressure by the reaction consumption is never compensated and the ratio of hydrogen to hydrocarbon remains uncertain after the beginning of the experiment.

If a sampling system is required, it should cool down immediately the samples once they leave the reactor. Another cooling system is needed to stop the reaction to proceed in the vessel when the experiment is completed.

This is a simple process diagram and it is not the only possible configuration. Changes can be made depending on the additional services available at installation site or special requirements of the process.

Gas effluent from the plant contains hydrogen sulfide as product of the reaction which must be neutralized prior venting or another operation. It is highly advisable to use a solution of NaOH and NaOCl in a packed scrubber to eliminate the acid effluent of the process. The packing will allow a better performance of the scrubber since it will increase the contact area between phases. The scrubber should be cleaned periodically especially if a continuous operation is performed to avoid the growth of bacteria [96,97].

5.3.2. Configuration of the experimental rig for continuous operation

The continuous mode requires more control of the inlet and outlet streams. Fig. 9 shows a simplified diagram of the configuration of the experimental setup in continuous operation. Flow meters are located at inlet and outlet streams and they should provide a mass flow rate reading in order to reduce the error due to changes in temperature and pressure of the stream. Liquid stream contains the catalyst in suspension so the process equipment should not be affected by the introduction of solids in the system especially at the measuring devices. A tank is needed for feeding the mixture of heavy oil and catalyst to the reactor and one more for product collection. Before entering the reactor both streams should be conditioned to reaction pressure and temperature. The streams can be mixed in the reactor or before the reactor but in this case a mixing device should be installed. Static mixers are preferred but simpler devices like tees might be used instead, if enough distance between the mixing point and the subsequent operation is allowed.

Once the reacting mixture leaves the reactor, it enters to a gas–liquid separator. After leaving the separator, gas and liquid

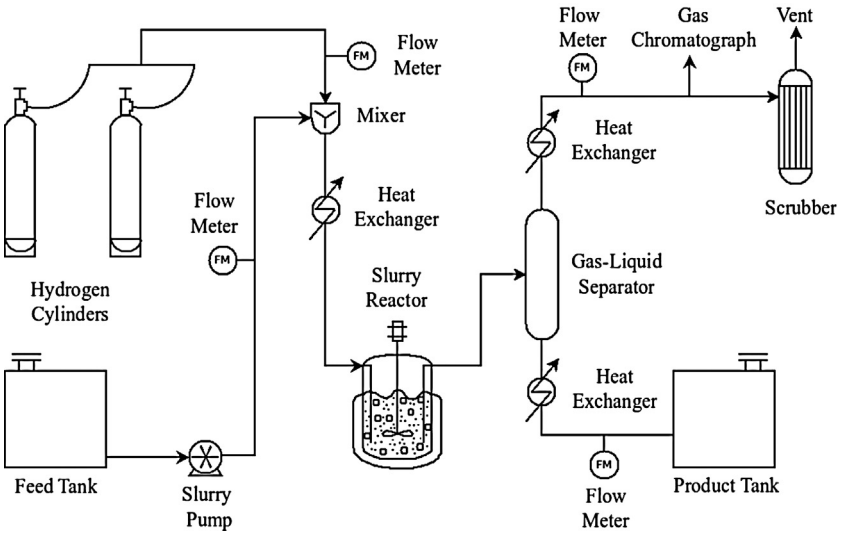

Fig. 9. Diagram of the experimental rig for hydrocracking of heavy oil in continuous operation mode.

should be conditioned for storage and analysis. It is worth to point out that liquid product can block process lines if operation temperature is close to ambient. On the other hand, gas should be analyzed online to minimize any error in the mass balance of the system. A simulation of the system should be able to identify the product distribution and expected flow rate of the streams. The latter is useful to identify the amount of light hydrocarbons that are dissolved in the liquid effluent and the amount and distribution of hydrocarbons that abandon the separator with the gas stream and which might not be analyzed by the gas chromatograph.

6. Manipulation of products after and catalyst reaction

6.1. Separation of products

A general flow diagram since the experiment is started as far as the product samples (hydrocracked products: gases and liquids) and a solid fraction (catalytic micrometer particles, and coke if produced) are recovered, is presented in Fig. 10. Liquid and gas products and catalysts are collected. The way to obtain samples depends on the reaction system employed. Generally, the liquid and solid fractions samples are recovered in an organic solvent (e.g. THF, toluene, CH_2Cl_2, etc.). The mixture is subsequently washed, centrifuged (12,000 rpm for 30 min) and separated by filtration through a millipore filter [6,98–102]. The reactor and the stirrer are usually washed with toluene which is recovered as well. The solid residue, which contains the catalyst, is washed with an organic solvent (n-heptane) to recover any oil and solid product. The solid fraction is dried, weighed and submitted for analysis. If toluene is used, the toluene insoluble (coke) is separated and extracted with boiling toluene, and the toluene soluble sample is distilled into several fractions [103]. The coke is isolated by adding toluene (10:1 by weight) followed by centrifugation at 3000 rpm for 20 min. The last procedure is repeated once more and, after filtration using a medium size fritted glass, the solid is dried at 75 °C for 2 h [104]. Finally, the gas phase products are either collected in sampling bags [99], or analyzed by online gas chromatograph (GC). In the latter, gas samples are periodically injected online in the GC. In some cases, there are two GCs online, the first one is used exclusively to quantify hydrogen while the second is used to determine the gas composition in order to estimate the average molecular weight of the light hydrocarbons (mainly C_1–C_5) contained in the gas phase.

6.2. Analysis of products

Different analytical procedures are carried out in order to determine the composition, properties and/or characteristics of the hydroprocessing reaction products and catalysts.

6.2.1. Gases

The quantification of gas phase products (H_2, H_2S, and C_1–C_5 hydrocarbons) is carried out in a gas chromatograph. Chemical species are separated in molecular sieves columns and identified by a thermal conductivity detector (TCD) and flame ionization detector (FID) [101,105–107]. The most common setups used of analysis of gases are described in Table 6.

6.2.2. Liquids

Liquid oil fraction is recovered from the reactor and separated from catalysts for subsequent analysis. The purpose is to obtain valuable information about the boiling range distribution, elemental composition (C, H, O, N and S), metal content (Ni and V) and for determining properties such as viscosity, API gravity, etc. The different techniques and analysis employed for the characterization for liquid oil product are presented in Table 7.

6.2.2.1. Boiling range distribution. The oil fraction product is commonly analyzed by GC temperature simulated distillation (SIM-DIST) and/or high temperature simulated distillation (HTSD).

SIM-DIST is probably the most useful analytical method for its ease and rapidity. This technique allows the elution of hydrocarbons containing up to 120 carbon atoms, using capillary columns with standing temperature up to 440 °C [108]. This technique serves to identify pseudocomponents distinguished by their boiling points for instance naphtha (IBP-216 °C), distillates (216–343 °C), vacuum gas oil, VGO (343–545 °C), and residue (545 °C+), according to ASTM D2887 method.

High-temperature simulated distillation (HTSD) using GC is based on the determination of the true boiling point (TBP) distribution of petroleum products up to a final boiling point (FBP) of 720 °C and it is recommended for analysis of samples containing distillation residua. It uses thermally stable wide bore capillary columns which have certain advantages over packed columns such as: better column stability and life, lower column bleed, faster analysis, elution of higher boiling petroleum fractions, compatibility

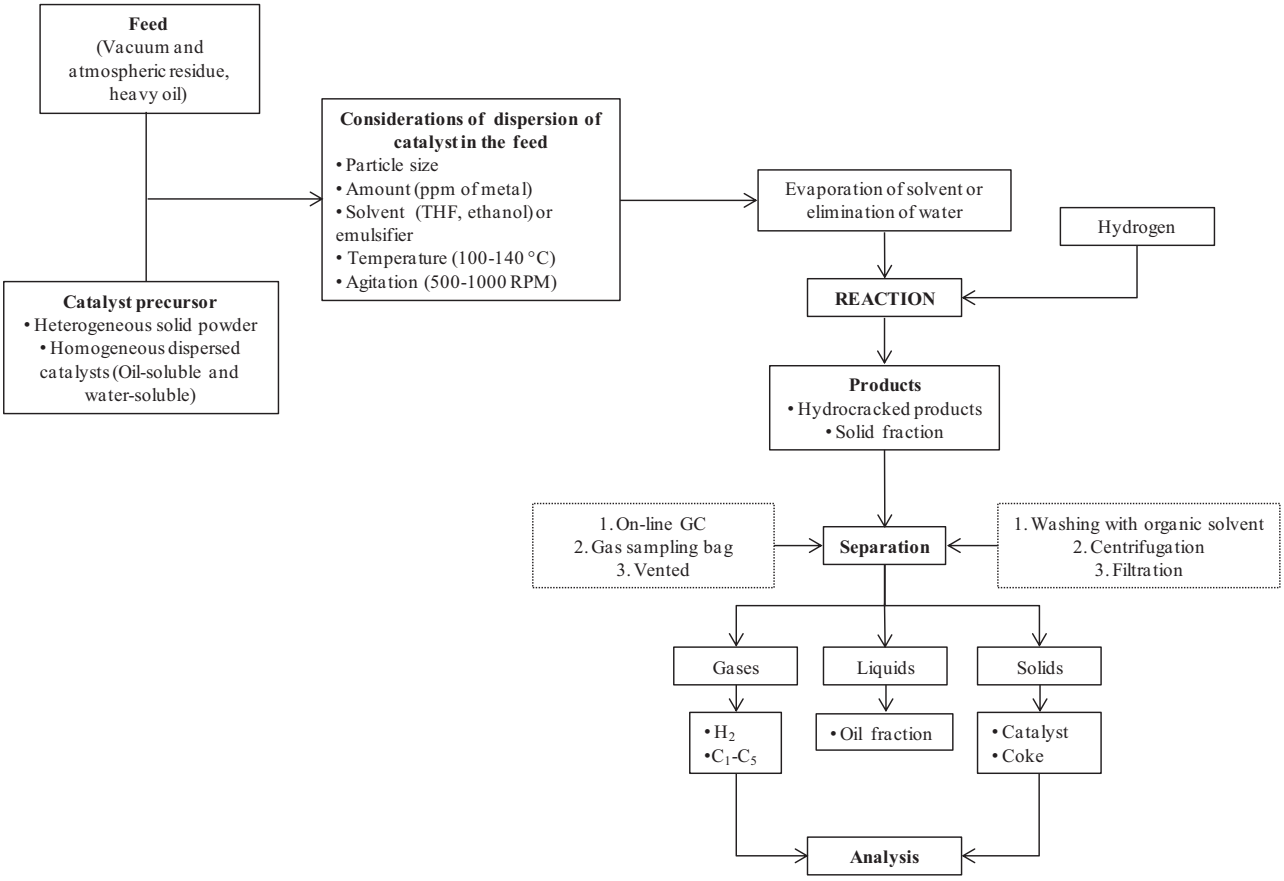

Fig. 10. Flow diagram of a hydrocracking experiment using dispersed catalyst.

with automated on-column injection, and improved reproducibility [109].

Reddy et al. [110] had developed an HTSD method where the atmospheric equivalent boiling points (AEBP) can reach an end point of 847 °C. Carbognani et al. [111] have reported an HTSD method based on the ASTM D-7169-2005 procedure, which was used to assess the cuts distributions and residue amount in the feedstock and liquid products obtained after its upgrading. Nowadays, the ASTM D-7169-11 method extends the boiling point profile up to 720 °C (corresponding to the elution of *n*-C_{100}), targeting at high boilers that do not easily elute out of a GC column.

6.2.2.2. Elemental analysis. The analysis of petroleum to determine the percentages of carbon, hydrogen, nitrogen, oxygen, and sulfur is perhaps the first method used to examine the general nature, and perform an evaluation, of a feedstock and hydrocracked products. The analyses are carried out in an elemental analyzer (CHN-2000 from LECO [112]) according to ASTM methods. The atomic ratios of the various elements to carbon (that is, H/C, N/C, O/C, and S/C) are frequently used as indicators of the overall character of the feedstock and products. It is also of value to determine the amounts of trace elements, such as vanadium and nickel, in a feedstock since these materials can have serious deleterious effects on catalyst performance during refining by catalytic processes [113]. The ASTM methods for ultimate elemental analysis of petroleum products are illustrated in Fig. 11.

6.2.2.3. Metal content. Metals (particularly vanadium and nickel) cause problems because they poison catalysts used for hydrotreating and hydrocracking, as well as other processes, such as catalytic cracking. Thus, serious attempts are being made to develop catalysts that can tolerate a high concentration of metals without

Table 6
GC used for analysis of gases after hydrocracking reaction.

Author	GC
Kennepoh and Sanford [101]	GC-4000A Beijing East & West Analytical Instruments, Inc. equipped with TCD and FID detectors
Dehkissia et al. [106]	GC-4000A Beijing East & West Analytical Instruments, Inc. equipped with TCD and FID detectors
	HP 5890 unit with TCD detector, and two columns. One packed with molecular sieve 13X and 1.8 m long, to analyze H_2, N_2, Ar, CH_4 and CO. The second, a 2.3 m long Porapak Q column, to quantify CO_2, H_2S, and C_2–C_5 hydrocarbon.
Siewe and Ng [107]	Perkin-Elmer GC model 8500 with TCD detector, with a carrier gas of 8.5% H_2 in He
Galarraga and Pereira-Almao [114]	GC Agilent model micro-GC 3000 for H_2 and a Hewlett-Packard 6900 GC for C_1–C_5 hydrocarbons with a 50 m length capillary column for PONA characterization
Rezaei et al. [120]	Varian Star 3400 CX GC with a 30 m capillary column (0.53 mm i.d.) and a TCD detector, and a HP 5890A GC with FID detector for C_1–C_4 gases using a 5 m long Porapak Q packed column
Del Bianco et al. [127]	Hewlett-Packard GC equipped with two TCD detectors and Poropak Q and molecular sieves columns
Xu et al. [133]	Agilent 6890 GC
Matsumura et al. [138]	GL Science model D7500

Table 7
Type of catalyst employed with specific feed and the products recovery and their analysis and/or set up employed for analysis.

Reference	Feed, catalyst and/or catalyst precursor	Recovery of liquids products	Analysis and/or equipment
[146]	Low sulfur waxy residue oil; water soluble Ni-Mo catalyst (nickel chloride and ammonium molybdate in 0.5 molar ratio)	Reactor cooled down to room temperature and purged with nitrogen at end of run and liquid product oil collected for analysis	Viscosity by viscometer model DV-111 Rheometer (M/S Brookfield Engineering Laboratories); elemental analysis by PE2400 Series II CHNS Element Analyzer (M/S Perkin Elmer); boiling range distribution by ASTM distillation
[99,126]	Vacuum residue of Belayim crude (10 g); molybdenum naphthenate, molybdenum acetyl acetonate, phosphomolybdic, acid, iron naphthenate, nickel naphthenate, cobalt resinate, vanadium resinate, ruthenium acetyl acetonate. Concentration: 1000–5000 ppm of metal; size: microsized powdered	Liquid and solid products of reactions recovered with THF. This mixture is stirred in ultrasonic bath for 15 min and filtered through a Millipore Teflon filter (0.5 mm) to separate THF-soluble material from residues (coke and metal catalyst)	Boiling range distribution by GC simulated distillation; sulfur content of distillate by GC system equipped with atomic emission detector (GC AED)
[138]	Brazilian Marlim vacuum residue (50 g); natural Australian and Brazilian limonites (active iron catalyst). Amount: 1.5 g of catalyst; size <150 μm	Oil fraction and solid residue separated by vacuum filtration	Gas chromatographic distillation by high temperature (Shimadzu GC-17A) equipped with wide-bore capillary column (GSE, HT-5), 12 m length with a 0.15-mm film thickness. The oven heated from 50 to 400 °C at 10 °C/min
[149]	Gudao vacuum residue; molybdenum dithiocarboxylate, Fe naphthenate, Co naphthelate. Concentration: 500 μg/g	Slurry centrifuged and toluene insoluble (coke) separated and extracted with boiling toluene. Toluene soluble distillated in several fractions	Elemental analysis (C, H, N, S); SARA analysis
[133]	Karamay vacuum residue (380 g); Co, Ni and Fe naphthenate, phosphomolybdic acid, ammonium molybdate tetrahydrate, cobalt nitride, ferric nitride, ferrous sulfate, nickel nitride and ammonium tungstate. Emulsifiers: Span 80 and Tween 80. Concentration: 500 μg/g catalyst (based metal in catalyst). Microsized powdered (finely)	Reactor cooled down to room temperature and purged with nitrogen at end of run. Liquid product oil (350 °C+) collected for analysis. Reactor and stirrer washed with toluene, and oil–toluene washings recovered	Viscosity by a rotary viscometer model DT500 (Haake Mess Technik Company); residue carbon concentration by electrical furnace method; boiling range distribution by GC simulated distillation
[125]	Liaohe atmospheric residue (350 g), nickel sulfate ($NiSO_4{\cdot}6H_2O$)	Oil sample diluted with certain amount of toluene and centrifuged in LD5-2A centrifuge at 3000 rpm. Light components of supernatant liquid (<360 °C) removed by vacuum distillation, and remaining fraction used for colloidal stability analysis	Oil samples analyzed for SARA components. Asphaltene fraction isolated by addition 30:1 ml of *n*-heptane/g sample, and maltenes fractioned into saturate, aromatic, and resin by liquid chromatography
[114]	Athabasca bitumen (30 g); Ni acetate, ammonium metatungstate, and ammonium heptamolybdate. Emulsifiers: Span 80 and Tween 80. Concentration: 1000 ppm (of metal with respect to the bitumen to produce atomic metallic ratios as follows: Ni/metals atomic = 0.3 and Mo/W atomic = 3, where metals = Ni + W + Mo). Size: submicronic	After reaction, the unit is allowed to cool before collecting samples	Water content by Karl Fischer titration method in a Mettler–Toledo model DL-32; viscosity at 40 °C by Brookfield viscometer model DV-III; The amount of residue 545 °C+ by HTSD (ASTM D-7169-2005 in a GC from Agilent modified (Separation Systems, Inc.); standard analyses to determine C and H performed in LECO apparatus; S content by UV fluorescence in an Antek model 9000NS
[143]	Cold Lake Vacuum Residue (80 g); ammonium heptamolybdate molybdenum chloride. Concentration: 100, 300, 600, 900 and 1800 ppm of Mo	Solid and liquid products recovered and separated using a Beckman Coulter Allegra 25R refrigerated centrifuge	HTSD using standardized UOP methodology; elemental analysis (C, H, N, S)

serious loss of catalyst activity or life. A variety of tests (ASTM D-1026, ASTM D-1262, ASTM D-1318, ASTM D-1368, ASTM D-1548, ASTM D-1549, ASTM D-2547, ASTM D-2599, ASTM D-2788, ASTM D-3340, ASTM D-3341, and ASTM D-3605) has been designated for the determination of metals in petroleum products. Determination of metals in whole feeds can be accomplished by combustion of the sample so that only inorganic ash remains. The ash can then be digested with acid and the solution is examined for metal species by atomic absorption (AA) spectroscopy or inductively coupled argon plasma (ICAP) spectrometry [113]. The methodology for metal determination includes: sample preparation, samples digestion and metal quantification.

Microwave ovens are commonly used for digesting, dissolving, hydrolyzing, extracting or drying a wide range of materials for AA and/or ICAP analysis.

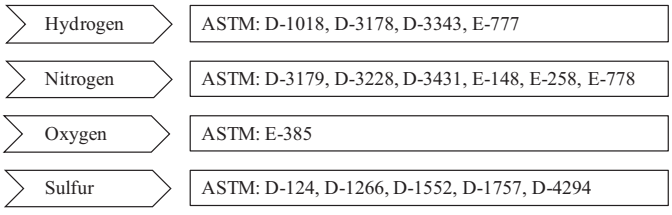

Fig. 11. ASTM methods used for determining H, N, O and S.

6.2.2.4. SARA composition. The four SARA-fractions are saturates (S), aromatics (A), resins (R) and asphaltenes (A). The SARA fractionation method usually starts with the removal of asphaltenes by precipitation with a saturated hydrocarbon (*n*-pentane or *n*-heptane) [100,114] as described by the ASTM D-3279 method [115]. The following SAR separation is then accomplished by elution with a series of increasingly polar solvents as mobile phases according with ASTM 2700 method, obtaining in this way the concentration of resins, aromatics and saturates [116,117]. Saturates are eluted first

Table 8
Analysis methods used for determining SARA composition.

Component	Method	Treatment
Saturates	ASTM D-4124	n-C_7 as solvent in a column packed with alumina
	ASTM D-2007	n-C_5 as solvent in a column packed with silica/clay
Aromatics	ASTM D-4124	Toluene as solvent in a column packed with alumina
Resins	ASTM D-4124	Methanol/toluene (1/1) and trichloroethylene in a column packed with alumina
Asphaltenes	ASTM D-893	n-C_5 as solvent at 65 ± 5 °C, centrifugation for 20 ± 1 min
	ASTM D-4124	n-C_7 as solvent at boiling point temperature and stirring for 1 h

with a non-polar solvent such as hexane, followed by the elution of the aromatics with toluene, and finally the resins are separated with a more polar solvent (Table 8). The SARA-separation can provide information somewhat between the one obtained by elemental analysis and the analysis of individual molecules [118].

6.2.2.5. Viscosity. Viscosity appears to be the most important physical property of heavy feeds. A sufficiently low viscosity has to be maintained to ensure adequate pumpability [119].

The ASTM methods developed for the determination of viscosity are: ASTM D-445, ASTM D-88, ASTM D-2161, ASTM D-341, and ASTM D-2270.

Many types of instruments have been proposed for obtaining viscosity, the simplest and most widely used are capillary types (ASTM D-445). Not only are such capillary instruments the most simple, but when designed in accordance with known principles and used with known necessary correction factors, they are probably the most accurate viscometers available. It is usually more convenient, however, to use relative measurements, and for this purpose the instrument is calibrated with an appropriate standard liquid of known viscosity [113].

6.2.3. Solids: catalyst and coke

The characterization techniques mainly used for the analysis of the catalyst and coke are X-ray diffraction (XRD) and scanning and transmission electron microscopy (SEM and TEM, respectively) [104,120], various examples are presented in Table 9. The samples for scanning electron microscopy (SEM) analysis are prepared by dispersing the filtered dry powder of residue in isopropyl alcohol, sonicating and dropping the dispersion on a glass disk. Most of the samples are prepared starting from the reaction products without separation by filtration [98,99,121].

7. The catalyst in dispersed phase

Compared with supported catalysts, highly dispersed catalyst particles suspended in heavy oil are less susceptible to deactivation during heavy oil upgrading. The advantages of unsupported dispersed catalysts over conventional supported catalysts for processing heavy feedstocks include elimination of catalyst pore plugging issues, increasing the accessibility of highly dispersed active sites by large size reactant molecules and minimizing diffusion control process during the reaction [101]. The use of these catalysts at relatively high temperatures causes fewer problems

Table 9
Characterization techniques and/or set ups for analysis of dispersed catalysts.

Catalyst	Characterization set ups and/or techniques	Reference
Phosphomolybdic acid; Mo, Ni, Co, and Fe naphthenates; Ruthenium acetylacetonate	XRD; HRTEM; STEM-EDX	[147]
Haematite; magnetite; pyrite; pyrrhotite	XRD: phase composition by DRON-3 diffractometer with graphite-monochromated Cu Kα radiation (λ = 1.54178 Å); HRTEM: REMMA-202 with X-ray microanalysis	[121]
Mo, Ni, Fe and Co naphthenate; Mo acetyl acetonate; phosphomolybdic acid; Ru acetyl acetonate	XRD: Philips goniometer, step scan method and Ni-filtered Cu Kα radiation (λ = 1.54178 Å), with DIFFRAC-500 computer package; SEM: Jeol JSM 840A microscope using a Kontron IBAS 2000 automatic image analyzer for particles with diameter greater than 0.1 mm; TEM: Philips 420T microscope equipped with an EDAX PV9900 EDS apparatus and operating at 100 kV	[99,126]
Iron dispersed catalyst derived from $Fe_3(CO)_{12}$	TEM: ISI equipment model SS-40 coupled with an EDAX X-ray analyzer model 9100; XPS: Leybold–Heraeus surface analysis system operated with an Al anode (1486.6 eV); Mössbauer spectroscopy: constant acceleration spectrometer, in the triangular symmetric mode for the velocity and a source of ^{57}Co in Pd	[148]
Nickel dispersed catalyst	XRD: D/MAX-IIIA diffractometer, Cu Kα radiation (D1.54178 Å); SEM: DEL-1200 EX transmission electron microscope; elemental analyses: elemental analysis equipment (Varil EL-3) and on an atomic absorption spectroscometer (Hitachi Z800)	[100]
Trimetallic ultra dispersed catalysts containing Ni, W, and Mo	ESEM: Philips model XL-30 with energy dispersive spectrometry (EDS) acquisition and analysis software and EDAX Genesis Spectrum V5.2; TEM: Hitachi model H-7650 at 10 kV	[114]
Molybdenum (V) chloride ($MoCl_5$)	SEM: 120 keV Hitachi S-3000N microscope with a light element EDX detector, XRD: Rigaku Multiflex diffractometer using Cu Kα radiation (l = 1.5406 A), a scan range of 2θ from 10° to 90° with a step size of 0.04° and scan rate of 2°/min	[120]
MoS_2 catalysts prepared from Mo-octoate and Mo-micelle precursors	Elemental analysis: 2400 Perkin-Elmer CHNSO analyzer; BET surface areas: Micromeritics ASAP 2020 analyzer; NMR: Varian Inova 400 for ^{13}C cross-polarization magic angle sample spinning (^{13}C CPMAS) spectra and Bruker Avance 500 MHz; XPS: Leybold Max200 X-ray photoelectron spectrometer with an Al Kα X-ray source; TGA: TGA-50 thermogravimetric analyzer (Shimadzu, Japan); DRIFTS: Nicolet 4700 FTIR unit (Thermo Electron Corporation) at ambient temperature	[143]

Table 10
Most common transitions metal compounds precursors for dispersed catalysts.

Oil soluble	Water soluble
Molybdenum dithiocarboxylate	Cobalt nitride
Iron naphthenate	Nickel nitride
Cobalt naphthenate	Ferric nitride
Nickel naphthenate	Ammonium molybdate tetrahydrate (AMT)
Molybdenum naphthenate	Phosphomolybdic acid (PMA)
Iron pentacarbonyl	Ammonium tungstate (AT)
Mo and Ni acetylacetonates	Ammonium heptamolybdate (AHM)
Molybdenum 2-ethyl hexanoate	Ammonium tetrathiomolybdate (ATTM)

with agglomeration and pressure drop; they also have a good ability to block free radicals, thus reducing polycondensation reactions.

Catalysts for slurry-phase hydrocracking of heavy oil are classified as heterogeneous solid powder catalysts and homogeneous dispersed catalysts, the last are divided in water or oil-soluble compounds [122–125].

For homogeneous dispersed catalysts (oil and water soluble), transition metal compounds are used as catalyst precursors (Table 10). These metallic compounds are mainly conformed by molybdenum, cobalt, iron and nickel as naphthenates or multi-carbonyl compounds for oil soluble dispersed catalyst [6,104,125–129]. For water soluble dispersed catalyst the phosphomolybdic acid and ammonium molybdate are commonly used as precursors [103,104,130,131]. Whereas for heterogeneous solid powder catalysts, the most important components include $FeSO_4$, natural ore and pulverized coal [98,125,126].

The concentrations of catalyst precursors added to the feedstock are typically in a range of 20–1000 ppm of the metal basis. Generally, catalyst concentrations are kept low (around 50–250 ppm), and the major observable effect is a reduction in solids formation in the reactor. This fact was reported by Panariti et al. [126] who used a catalyst concentration of 0–5000 ppm (molybdenum naphthenate) at different levels of reaction severity. It was observed at any level of severity that coke formation increased at very high catalyst concentrations (5000 ppm of Mo). The results also showed that distillate production is not significantly affected by catalyst concentration and hydrogen pressure as is presented in Fig. 12. Similarly, Ortiz-Moreno et al. [131] studied the increment of catalyst loading from 330 to 1000 ppm Mo (using ammonium tetrathiomolybdate as precursor) for the hydrocracking of Maya crude oil, keeping the operating pressure at 800 psi and temperature of 390 and 400 °C. They observed that the catalyst loading (330 ppm Mo) and operating temperature can be tuned to improve the product distribution.

7.1. Treatment of catalyst and feed

The size and degree of dispersion of catalyst particles strongly affect its activity. The limitations of catalytic activity can be due to either the particle size of the active species formed in the reaction medium or to a poor distribution in the reacting mixture. Catalyst activity can be controlled by the temperature at which the active catalyst species is formed and selecting a particular precursor or mixtures of them. However, the solubility of the precursor may influence the particle size of the catalyst and its dispersion in the heavy crude oil. In fact, catalyst activity is controlled by the degree of dispersion and the composition of the catalyst under a given set of reaction conditions. A well-dispersed catalyst should favor rapid uptake of hydrogen due to the maximum interaction of oil and hydrogen. The interaction can occur on the high surface area of the small particles preventing free radical condensation that leads to coke formation [6,132]. These catalysts can be introduced into the feed as finely divided powders, water-soluble or oil-soluble precursors whose thermal decomposition produced micrometer-sized particles of the active species [127,133].

For this reason, hydrotreatment processes utilizing dispersed catalysts are particularly suited for upgrading heavy oils and

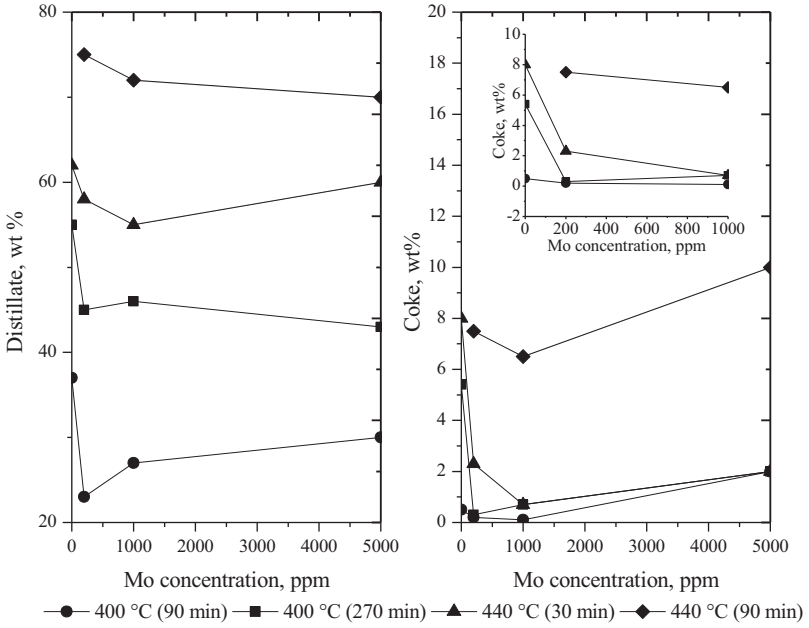

Fig. 12. Effect of molybdenum concentration on distillates and coke yields at different levels of severity: pressure of hydrogen of 8 MPa, 400 °C (90 min), 400 °C (270 min), 440 °C (30 min) and 440 °C (90 min) [126].

Table 11
Metal precursors soluble in ethanol.

Precursor type	Manufacturer	Metal (wt%)
Molybdenyl acetylacetonate	Shepherd	Mo (29.4)
Phosphomolybdic acid	Aldrich	Mo (64.0)
Phosphotungstic acid	Aldrich	W (75.3)
Nickel acetylacetonate	Strem	Ni (19.3)
Cobalt acetylacetonate	Aldrich	Co (19.3)

residual oils which contain high concentration of metallic contaminants, asphaltenes, sulfur and nitrogen compounds, and high Conradson carbon residue.

7.1.1. Particle size of catalyst

Dispersed catalysts require a special treatment before being incorporated to the feed. The catalysts must be reduced in size, due to the inter-particle distance is an important factor for the hydrocracking reaction. The free radical intermediates produced must react immediately and be hydrogenated to prevent the formation of coke and incompatible polymeric oils [134]. Microsized materials can be obtained by various techniques, such as laser pyrolysis, plasma methods, chemical synthesis such as microemulsion [99,132,135] and also mechanical techniques [135,136]. Mechanical techniques are classified as dry milling, wet milling and high pressure homogenization. The wet-media milling, piston gap homogenization and microfluidization are employed to obtain particles in the submicron (nano) range and to further increase the solubility in the media [137]. It has been found that the particle size is in a range from sub-micron to several microns, generally, less than 150 μm [100,104,121,130–140] and some authors have even mentioned particles less than 1 μm [127].

In the case of water–oil soluble catalyst, the size of the micelle, and consequently the size of the particle formed in its core, is easily controlled by varying the water to surfactant ratio. When the ratio of water and oil is kept at fixed values, an enhancing in the amount of surfactant increases the number of droplets, which decreases the number of metal ions per droplet and therefore the particle size [141].

7.1.2. Dispersion of catalyst in the feed

Highly dispersed catalyst particles suspended in heavy oil are less susceptible to deactivation during heavy oil upgrading and they offer better contact with the reactants than the supported catalysts. The dispersion of catalyst can be significantly improved by reducing the interfacial tension between the precursor solution and the feedstock [140–143].

The oil-soluble catalyst precursors are well-dispersed in residue and have high activity, therefore, oil-soluble metal precursor as catalysts have become popular. Commonly, the precursor can be introduced directly into the feedstock, or it may be mixed with a suitable solvent (oil or water), and then be combined with the hydrocarbon feedstock. In order to disperse the oil-soluble catalyst precursor in source oil, the desired concentration of the metallic precursor is mixed with heavy oil in a stirred heated tank at around 1000 rpm [6]. In some cases, in order to have an effective dispersion in the feedstock, organic solvents such as tetrahydrofuran (THF) and ethanol are used. In this case, the solution is strongly mixed for several minutes (10–60 min) in a batch reactor equipped with a magnetically driven impeller. After this, the solvent is removed by rotary evaporation at 80–100 °C [4,98,128], or in the case where ethanol is employed the mixture is heated at 250 °C in a silicon oil bath and maintained at this temperature for 2 h for complete evaporation of ethanol from the oil [128]. Some metallic precursors soluble in ethanol are illustrated in Table 11.

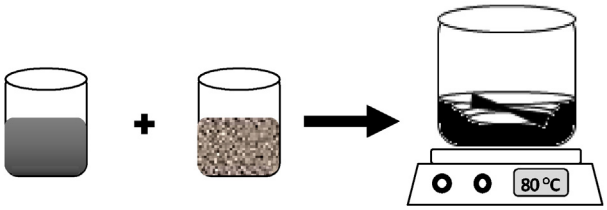

Fig. 13. Integration of dispersed catalyst and emulsifier to the heavy crude oil.

Because oil-soluble dispersed catalysts are expensive, water-soluble dispersed catalysts are widely investigated in slurry-phase hydrocracking of heavy oil. When water-soluble precursors are used (ferrous salts, nickel salts, or molybdates), aqueous solution and emulsifier (commonly Tween 80 and Span 80) are added to the feedstock using a slurry stirrer as dispersion media [133,144,112]. The mixture is heated at around 50–80 °C, a small slurry blender is used to stir the feed oil during the period of catalyst solution addition, which is usually 20–80 min. Then the solution of catalyst precursor is added dropwise, stirred at 500–4000 rpm (Fig. 13). After stirring, the mixture is heated to 80–180 °C and bubbled with nitrogen to remove the water [100,129,133,36]. Here, it is significant to consider that the temperature plays an important role into the system, since it is strongly sensitive to decomposition temperature, particularly in the case of non-ionic surfactants.

In this respect, Xu et al. [133] have studied the catalytic activity of finely oil and water soluble dispersed catalysts for upgrading Karamay vacuum residue using syngas. The catalysts were prepared by means of microemulsion. The tests were carried out in a batch-type autoclave under the following process conditions: reaction temperature of 420 °C, residence time of 1 h, pressure of 6 MPa, catalyst content of 500 ppm. The activities of several high performance catalysts obey this order: Mo/Co > Mo/Ni > CoNaph > NiNaph > $Co(NO_3)_2$ > $Ni(NO_3)_2$ > AMT, as is presented in Fig. 14.

7.1.3. Sulfurization of the catalyst precursor

Sulfurization remarkably affects the physical and chemical properties of dispersed catalysts. The dispersed metal reacts with the sulfur contained in the heavy oil to form the active catalyst species [36]. Once the catalyst precursor is added to the feedstock, the mixture is stirred to disperse completely the catalyst precursor in the source oil. Meanwhile the solution of the sulfiding reagent is added to the solution of feedstock and catalyst and then heated to form the catalytic active species [129]. The water soluble precursor can react with the water-soluble sulfides in solution; thus, it may be more appropriate to perform the sulfurization based on these reactions [129,145].

When the catalyst is activated by addition of a sulfur compound, it is necessary to incorporate an excess of the sulfiding agent. That is usually three-fold of the amount needed for the sulfiding of the metals [99,104]. For this intermediary step, it is necessary to take into account [103,127,133,140]:

(1) The amount of precursor that is obtained from the ratio of metal weight that is contained in the feedstock oil (S/metal atomic ratio = 3).
(2) The amount of sulfurizer agent which is calculated from the molar ratio of the sulfur content to the amount of metal that the precursor contains.

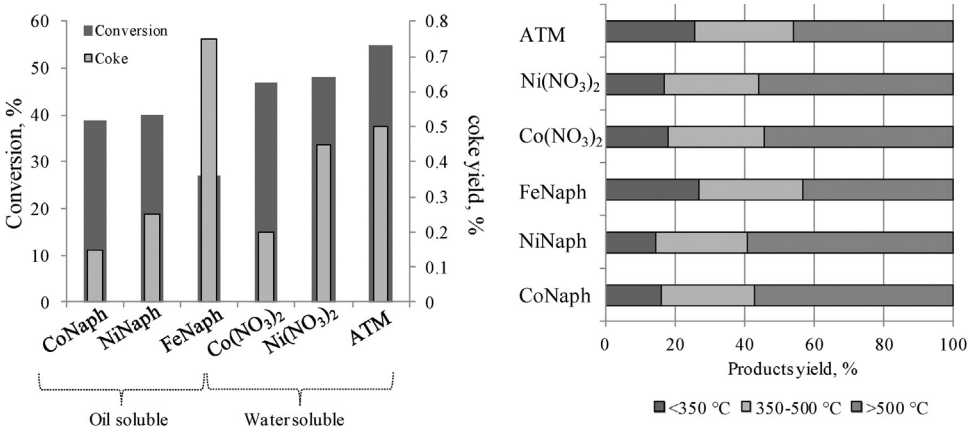

Fig. 14. Conversion and product yields obtained using different type of catalyst (Mo/Co, Mo/Ni, CoNaph, NiNaph, $Co(NO_3)_2$, $Ni(NO_3)_2$, AMT) at 420 °C, residence time of 1 h, pressure of 6 MPa, catalyst content of 500 ppm [133].

(3) The amount of auxiliary sulfurization reagent is marked by the molar ratio of auxiliary sulfurization reagent to metal element in the precursor catalyst (five times the stoichiometric).

8. Concluding remarks

A thorough description of the experimental aspects involved in the study of hydrocracking of heavy oil reactions with dispersed catalysts was reviewed and discussed.

Chemical kinetics aspects of the reaction were treated in order to establish the elementary steps involved during the reaction process. A series of experimental tests were organized to identify a region of operating conditions where the chemical reaction is the controlling mechanism.

Advantages and disadvantages of the different operation modes of experimental rigs were highlighted. The selection of any particular mode of operation obeys basically to economical and safety aspects. Operation in batch mode is preferred since it requires the minimum amount of laboratory equipment and represents the lowest safety risks.

According to the type of reaction, three types of reactors were found suitable to study the hydrocracking reaction (stirred tank reactors, bubble column and three-phase fluidized bed reactor). The information provided is centered (but not limited) to the stirred tank reactor since they are commonly found in laboratory. Operational aspects to assure an optimal reactor performance in a three-phase reaction were covered. Dimensioning of the internal configuration of stirred tank was detailed together with the calculation of the minimum agitation speed needed for a complete suspension of the catalyst particles. Optimal operational gas velocity needed to maintain a homogeneous regime of operation and a complete suspension of the catalyst were provided through a series of equations for bubble column and three-phase fluidized bed reactors.

A list of the most common analytical techniques to quantify gas and liquid samples besides solid (products and catalysts) characterization was presented.

Important factors such as catalyst pretreatment, particle size, catalyst dispersion and catalyst sulfurization were also commented. These factors together with the reactor performance are responsible for the development of the reaction.

Separation and analytical techniques to characterize gas, liquid and solid samples were also covered.

The information presented in this paper is intended to serve as guide for the development of experimental research in the area of heavy oil hydrocracking using dispersed catalysts.

Acknowledgments

M.J. Angeles expresses his deep gratitude to Consejo Nacional de Ciencia y Tecnología (CONACYT), México for the financial support provided for this research. The authors thank Instituto Mexicano del Petróleo for the financial support.

References

[1] J. Ancheyta, Modeling of Processes and Reactors for Upgrading of Heavy Petroleum, CRC Press Taylor and Francis Group, Boca Raton, 2013.
[2] J. Ancheyta, J.G. Speight, Hydroprocessing of Heavy Oils and Residua, CRC Press Taylor and Francis Group, Boca Raton, 2007.
[3] D.S.J. Jones, P.R. Pujadó, Handbook of Petroleum Processing, first ed., The Netherlands, Springer, 2008.
[4] Y. Liu, L. Gao, L. Wen, B. Zong, Recent Pat. Chem. Eng. 2 (2009) 22–36.
[5] R.V. Chaudari, P.A. Ramachandran, AIChE J. 26 (1980) 177–201.
[6] D. Liu, M. Li, W. Deng, G. Que, Energy Fuel 24 (2010) 1958–1962.
[7] H. Hassanzadeh, J. Abedi, Fuel 89 (2010) 2822–2828.
[8] K. Østergard, Adv. Chem. Eng. 7 (1968) 71–131.
[9] R. Klaewkla, M. Arend, W.F. Hoelderich, A review of mass transfer controlling the reaction rate in heterogeneous catalytic systems, in: H. Nakajima (Ed.), Mass Transfer—Advanced Aspects, InTech, Rijeka, 2011, pp. 667–684.
[10] G. Astarita, Mass Transfer with Chemical Reactions, Elsevier, Amsterdam, 1967.
[11] G.K. Patterson, E.L. Paul, S.M. Kresta, A.W. Etchells III, Mixing and chemical reactions, in: E.L. Paul, V.A. Atiemo-Obeng, S.M. Kresta (Eds.), Handbook of Industrial Mixing. Science and Practice, John Wiley and Sons, New Jersey, 2004, pp. 755–868.
[12] L.K. Doraiswamy, M.M. Sharma, Heterogeneous Reactions: Analysis, Examples and Reactor Design, Volume II, Fluid–Fluid–Solid Reactions, John Wiley and Sons, New York, 1984.
[13] J. Ancheyta, S. Sánchez, M.A. Rodríguez, Catal. Today 109 (2005) 76–92.
[14] S. Foggler, Elements of Chemical Reaction Engineering, fourth ed., Prentice Hall, New Jersey, 2005.
[15] C.N. Satterfield, Mass Transfer in Heterogeneous Catalysis, MIT Press, 1970.
[16] P. Trambouze, H. Van Landeghem, J.P. Wauquier, Chemical Reactors Design/Engineering/Operation, Gulf Publishing Company, Houston, 1984.
[17] E. Santacesaria, M. Di Serio, P. Iengo, Catal. Today 52 (1999) 363–376.
[18] H.S. Davis, G. Thomson, G.S. Crandall, J. Am. Chem. Soc. 54 (1932) 2340–2350.
[19] T.K. Sherwood, E.J. Farkas, Chem. Eng. Sci. 21 (1966) 573–582.
[20] E.L. Cussler, Diffusion Mass Transfer in Fluids Systems, third ed., Cambridge University Press, Cambridge, 2009.
[21] P. Harriott, Chemical Reactor Design, Marcel Dekker, Inc, New York, 2003.
[22] G. Biardi, G. Baldi, Catal. Today 52 (1999) 223–234.
[23] E. Santacesaria, P. Wilkinson, P. Babini, S. Carrá, Ind. Eng. Chem. Res. 27 (1988) 780–784.
[24] E. Santacesaria, M. Di Serio, R. Velotti, U. Leone, Ind. Eng. Chem. Res. 33 (1994) 277–284.
[25] L.C. Castañeda, J.A.D. Muñoz, J. Ancheyta, Fuel 90 (2011) 3593–3601.
[26] H. Korsten, U. Hoffman, AIChE J. 42 (1996) 1350–1360.
[27] M. Mapiour, V. Sundaramurthy, A. Dalai, J. Adjave, Energy Fuel 23 (2009) 2129–2135.
[28] E. Apler, B. Wichtendahl, W.-D. Deckwer, Chem. Eng. Sci. 35 (1980) 217–222.
[29] R.V. Chaudari, P.A. Ramachandran, Ind. Eng. Chem. Fundam. 19 (1980) 201–206.
[30] N.D. Sylvester, A.A. Kulkarni, J.J. Carberry, Can. J. Chem. Eng. 53 (1975) 313–316.

[31] Y.T. Shah, B.G. Kelkar, S.P. Godbole, W.-D. Deckwer, AIChE J. 28 (1982) 353–379.
[32] N. Kantarci, F. Borak, K.O. Ulgen, Process Biochem. 40 (2005) 2263–3228.
[33] E. Dietrich, C. Mathieu, H. Delmas, J. Jenck, Chem. Eng. Sci. 47 (1992) 3597–3604.
[34] V. Meille, N. Pestre, P. Fongarland, C. de Bellefon, Ind. Eng. Chem. Res. 43 (2004) 924–927.
[35] M.M. Fathi, P. Pereira-Almao, Energy Fuel 25 (2011) 4867–4877.
[36] D. Liu, X. Kong, M. Li, G. Que, Energy Fuel 23 (2009) 958–961.
[37] A. Matsumura, S. Sato, T. Kondo, S. Sato, I. Saito, W. Ferraz de Souza, Fuel 84 (2005) 417–421.
[38] A. Nishijima, T. Sato, Y. Yoshimura, H. Shimada, N. Matsubayashi, M. Imamura, Y. Sugimoto, T. Kameoka, Y. Nishimura, Catal. Today 27 (1996) 129–135.
[39] M.S. Rana, V. Sámano, J. Ancheyta, J.A.I. Diaz, Fuel 86 (2007) 1216–1231.
[40] A. Gupta, D. Borssard, The hydroconversion of residues Encyclopedia of Hydrocarbons, vol. II Refining, Istituto della Enciclopedia Italiana, Rome, 2005, pp. 309–323.
[41] J.F. Kriz, M. Ternan, J.M. Denis, Hydrocarbon processing, Hydrocracking of bitumen and heavy Oils, 5th NCUT Upgrading and Refining Conference 2009, September 14-16, 2009, Edmonton, Canada.
[42] W. Deng, H. Luo, J. Gao, G. Que, Energy Fuel 25 (2011) 5360–5365.
[43] M. Millan, C. Adell, C. Hinojosa, A.A. Herod, D. Dugwell, R. Kandiyoti, Energy Fuel 21 (2007) 1370–1378.
[44] Y. Zhao, F. Wei, S. Zhang, Y. Yu, Fuel 90 (2011) 1900–1906.
[45] P.M. Rahimi, T. Gentzis, Fuel Proc. Technol. 80 (2003) 69–79.
[46] G. Gualda, S. Kasztelan, J. Catal. 161 (2006) 1996.
[47] B.B. Pruden, Can. J. Chem. Eng. 56 (1978) 277–280.
[48] W.-W. Pang, M. Kuramae, Y. Kinoshita, J.-K. Lee, Y.Z. Zhang, S.-H. Yoon, I. Mochida, Fuel 88 (2009) 663–669.
[49] J.G. Speight, Catal. Today 98 (2004) 55–60.
[50] A.K. Coker, Modeling of Chemical Kinetics and Reactor Design, Gulf Publishing Company, Boston, 2001.
[51] C.H. Bartholomew, W.C. Hecker, Chem. Eng. 101 (1994) 70–75.
[52] R.W. Missen, C.A. Mims, B.A. Saville, Introduction to Chemical Reaction Engineering and Kinetics, John Wiley and Sons, New York, 1999.
[53] V.W. Weekman, AIChE J. 20 (1974) 833–840.
[54] E.B. Nauman, Ind. Eng. Chem. Res. 47 (2008) 3752–3766.
[55] A.I. Stankiewicz, J. Moulijn, Chem. Eng. Prog. 96 (2000) 22–34.
[56] E.B. Nauman, D. Kothari, K.D.P. Nigam, T. I. Chem. Eng.-Lon. A 80 (2002) 681–685.
[57] R.K. Thakur, K.D.P. Nigam, E.B. Nauman, G. Djelveh, T. I. Chem. Eng.-Lon. A 81 (2003) 787–826.
[58] O. Levenspiel, Chemical Reaction Engineering, third ed., John Wiley and Sons, New York, 1999.
[59] I. Pitault, P. Fongarland, M. Mitrovic, D. Ronze, M. Forissier, Catal. Today 98 (2004) 31–42.
[60] E.B. Nauman, Chemical Reactor Design, Operation, and Scaleup, second ed., John Wiley and Sons, New Jersey, 2008.
[61] J. Baldyga, R. Pohorecki, Chem. Eng. J. 58 (1995) 183–195.
[62] M.O. Tarhan, Catalytic Reactor Design, McGraw-Hill Inc, New York, 1983.
[63] M. Zlokarnik, Stirring, in: Ullmann's Encyclopedia of Industrial Chemistry, Electronic release, Wiley-VCH, Weinheim, 2005, pp. 1–40.
[64] N.A. Deshmukh, S.S. Patil, J.B. Joshi, T. I. Chem. Eng.-Lon. A 84 (2006) 124–132.
[65] J.C. Middleton, J.M. Smith, Gas–liquid mixing in turbulent systems, in: E.L. Paul, V.A. Atiemo-Obeng, S.M. Kresta (Eds.), Handbook of Industrial Mixing. Science and Practice, John Wiley and Sons, New Jersey, 2004, pp. 585–638.
[66] V.A. Atiemo-Obeng, W.R. Penney, P. Armenante, Solid–Liquid mixing, in: E.L. Paul, V.A. Atiemo-Obeng, S.M. Kresta (Eds.), Handbook of Industrial Mixing. Science and Practice, John Wiley and Sons, New Jersey, 2004, pp. 543–584.
[67] P.A. Ramachandran, R.V. Chaudhari, Three Phase Catalytic Reactors, Gordon and Breach Science Publishers, Philadelphia, 1983.
[68] R.R. Hemrajani, G.B. Tatterson, Mechanically stirred vessels, in: E.L. Paul, V.A. Atiemo-Obeng, S.M. Kresta (Eds.), Handbook of Industrial Mixing. Science and Practice, John Wiley and Sons, New Jersey, 2004, pp. 345–390.
[69] G.R. Kasat, A.B. Pandit, Can. J. Chem. Eng. 83 (2005) 618–643.
[70] G. Baldi, R. Conti, E. Alaria, Chem. Eng. Sci. 33 (1978) 21–25.
[71] K.S.M.S.R. Rao, V.B. Rewatkar, J.B. Joshi, AIChE J. 34 (1988) 1332–1340.
[72] V.B. Rewatkar, K.S.M.S.R. Rao, J.B. Joshi, Ind. Eng. Chem. Res. 30 (1991) 1770–1784.
[73] V.B. Rewatkar, J.B. Joshi, Ind. Eng. Chem. Res. 30 (1991) 1784–1791.
[74] J.C. Middleton, K.J. Carpenter, Stirred-tank and loop reactors, in: Ullmann's Encyclopedia of Industrial Chemistry, Electronic Release, Wiley-VCH, Weinheim, 2005, pp. 1–14.
[75] M.M.P. Zieverink, M.T. Kreutzer, F. Kapteijn, J.A. Moulijn, Ind. Eng. Chem. Res. 45 (2006) 4574–4581.
[76] H. Hichri, A. Accary, J.P. Puaux, J. Andrieu, Ind. Eng. Chem. Res. 31 (1992) 1864.
[77] M. Bouaifi, G. Hebrard, D. Bastoul, M. Roustan, Chem. Eng. Proc. 40 (2011) 97–111.
[78] P. Zehner, M. Kraume, Bubble columns, in: Ullmann's Encyclopedia of Industrial Chemistry, Electronic Release, Wiley-VCH, Weinheim, 2005, pp. 1–34.
[79] E.G. Christoffel, Catal. Rev. Sci. Eng. 24 (1982) 159–232.
[80] M.P. Duduković, F. Larachi, P.L. Mills, Catal. Rev. Sci. Eng. 44 (2002) 123–246.
[81] T. Wang, J. Wang, Y. Jin, Ind. Eng. Chem. Res. 46 (2007) 5824–5847.
[82] J.-M. Schweitzer, S. Kressmann, Chem. Eng. Sci. 59 (2004) 5637–5645.
[83] E.M. Matos, R. Guirardello, Braz. J. Chem. Eng. 19 (2002) 319–334.
[84] M.M. Carbonell, R. Guirardelo, in: B. Delmon, G. Froment, P. Grange (Eds.), Modelling of Hydroconversion Reactors Based on a Computational Fluid Dynamics Approach in Hydrotreatment and Hydrocracking of oil Fractions, Elsevier, Amsterdam, 1999, pp. 289–296.
[85] E.M. Matos, J.R. Nunhez, Chem. Eng. J. 116 (2006) 163–172.
[86] G. Wild, S. Poncin, Three-Phase Sparge Reactors, Gordon and Breach Science Publishers, Amsterdam, 1996.
[87] A.V. Kulkarni, Chem. Eng. Tech. 33 (2010) 1015–1022.
[88] A.V. Kulkarni, J.B. Joshi, Chem. Eng. Res. Des. 89 (2011) 1972–1985.
[89] A.V. Kulkarni, J.B. Joshi, Chem. Eng. Res. Des. 89 (2001) 1986–1995.
[90] S.-Y. Lee, Y.P. Tsui, Chem. Eng. Prog. 95 (1999) 23–49.
[91] N.K. Roy, D.K. Guha, M.N. Rao, Chem. Eng. Sci. 19 (1964) 215–225.
[92] M. Immich, U. Onken, Chem. Eng. Sci. 47 (1992) 3379–3386.
[93] J. Martínez, J.L. Sánchez, J. Ancheyta, R.S. Ruiz, Catal. Rev. 52 (2010) 60–105.
[94] J.-P. Zhang, J.R. Grace, N. Epstein, K.S. Lim, Chem. Eng. Sci. 52 (1997) 3979–3992.
[95] F. Larachi, I. Iliuta, O. Rival, B.P.A. Grandjean, Ind. Eng. Chem. Res. 39 (2000) 563–572.
[96] L. Chen, J. Huang, C.-L. Yang, Environ. Prog. 20 (2001) 175–181.
[97] F.X. McConville, The Pilot Plant Real Book, FXM Engineering and Design, Massachussets, 2002.
[98] N. Rueda, R. Bacaud, P. Lanteri, M. Vrinat, Appl. Catal. A: Gen. 215 (2000) 81–89.
[99] N. Panariti, A. Del Bianco, G. Del Piero, M. Marchionna, Appl. Catal. A: Gen. 204 (2000) 203–214.
[100] Z. Shuyi, D. Wenan, L. Hui, L. Dong, Q. Guohe, Energy Fuel 22 (2008) 3583–3586.
[101] D. Kennepoh, E. Sanford, Energy Fuel 10 (1996) 229–234.
[102] B. Demirel, E.N. Givens, Fuel 79 (2000) 1975–1980.
[103] J. Cheng, Y. Liu, Y. Lou, G. Que, Petrol. Sci. Technol. 23 (2005) 1453–1462.
[104] D.K. Lee, W.L. Yoon, S.I. Woot, Fuel 75 (1996) 1186–1192.
[105] A. Del Bianco, N. Panariti, S. Di Carlo, P.L. Beltrame, P. Carnitii, Energy Fuel 8 (1994) 593–597.
[106] S. Dehkissia, F. Larachi, E. Chornet, Fuel 83 (2004) 1323–1331.
[107] C.-N. Siewe, F.T.T. Ng, Energy Fuel 12 (1998) 598–606.
[108] R. Bacauda, L. Rouleaua, V.L. Cebolla, L. Membrado, J. Vela, Catal. Today 43 (1998) 171–186.
[109] Hewlett-Packard Gas Chromatography Application Note 228-60, January 1988.
[110] K.M. Reddy, B. Wei, C. Song, Catal. Today 43 (1998) 187–202.
[111] L. Carbognani, J. Lubkowitz, M.F. Gonzalez, P. Pereira-Almao, Energy Fuel 21 (2007) 2831–2839.
[112] E. Peluso, Ph D. Thesis, Hydroprocessing full-range of heavy oils and bitumen using ultradispersed catalysts at low severity, University of Calgary, Canada, 2011.
[113] J.G. Speight, Feedstock evaluation and composition, in: J. Ancheyta, J.G. Speight (Eds.), Hydroprocessing of Heavy Crude Oils and Residua, CRC Press, Taylor & Francis Group, Boca Raton, FL, 2007, pp. 15–31.
[114] C.E. Galarraga, P. Pereira-Almao, Energy Fuel 24 (2010) 2383–2389.
[115] F. Trejo, G. Centeno, J. Ancheyta, Fuel 83 (2004) 2169–2175.
[116] D. Molina, U. Navarro-Uribe, J. Murgich, Fuel 89 (2010) 185–192.
[117] P. Luo, Y. Gu, Fuel 86 (2007) 1069–1078.
[118] J.G. Speight, J.G. The Chemistry, Technology of Petroleum, Marcel Dekker, New York, 1999.
[119] S.R. Al-Maamari, O. Houache, S.A. Abdul-Wahab, Energy Fuel 20 (2006) 2586–2592.
[120] H. Rezaei, X. Liu, S.J. Ardakani, K.J. Smith, M. Bricker, Catal. Today 150 (2010) 244–254.
[121] V.I. Sharypov, B.N. Kuznetsov, N.G. Beregovtsova, O.L. Reshetnikov, S.V. Baryshnikov, Fuel 75 (1996) 39–42.
[122] E. Furimsky, Catalysts for Upgrading Heavy Petroleum Feeds, Elsevier, Amsterdam, 2007.
[123] Y. Li, Y.J., Wang, L., Jiang, Z., Zhang, J., Liu, S., Ren, B., Zhao, Y. Jia, U.S. Patent 6004454, 1999.
[124] G. Que G, C., Men, C., Meng, A., Ma, J., Zhou, W., Deng, Z., Wang, B., Mu, C., Liu, D., Liu, S., Liang, B. Shi, U.S. Patent 6660157, 2003.
[125] Z. Shuyi, D. Liu, W. Deng, G. Que, Energy Fuel 21 (2007) 3057–3062.
[126] N. Panariti, A. Del Bianco, G. Del Piero, M. Marchionna, P. Carniti, Appl. Catal. A: Gen. 204 (2000) 215–222.
[127] A. Del Bianco, N. Panariti, S. Di Carlo, P.L. Beltrame, P. Carniti, Energy Fuel 8 (1994) 593–597.
[128] D.K. Lee, S.K. Park, W.L. Yoon, I.C. Lee, S.I. Woo, Energy Fuel 9 (1995) 2–9.
[129] R. Ren, Z. Wang, C. Guan, B. Shi, Fuel Process. Technol. 86 (2004) 169–178.
[130] P. Afanasie, C. R. Chim. 11 (2008) 159–182.
[131] H. Ortiz-Moreno, J. Ramírez, R. Cuevas, G. Marroquín, J. Ancheyta, Fuel 100 (2012) 186–192.
[132] A. Del Bianco, N. Panariti, J. Elmouchnino, B. Fixari, P. Le Perchec, Appl. Catal. A: Gen. 94 (1993) 1–16.
[133] Y. Xu, M. Yuan, S. Zhao, C. Xu, Petrol. Sci. Technol. 27 (2009) 712–732.
[134] A. Duangchan, Ph. D. Thesis, Residue upgrading using dispersed catalysts prepared in reverse micelles, University of Alberta, Canada, 1998.
[135] M. Boutonnet, J. Kizling, P. Stenius, Colloid Surf. A 5 (1982) 209–225.
[136] K. Hirano, M. Kouzu, T. Okada, M. Kobayashi, N. Ikenaga, T. Suzuki, Fuel 78 (1999) 1867–1873.
[137] J.O. Morales, A.B. Watts, J.T. McConville, Mechanical particle size reduction techniques, in: R.O. Williams III, A.B. Watts, D.A. Miller (Eds.), Formulating

Poorly Water Soluble Drugs, AAPS Advances in the Pharmaceutical Sciences Series, vol. 3, Springer, New York, 2012, pp. 133–170.
[138] A. Matsumura, T. Kondo, S. Sato, I. Saito, W. Ferraz de Souza, Fuel 84 (2005) 411–416.
[139] G. Noguera, S. Araujo, J. Hernández, A. Rivas, D. Mendoza, O. Castellano, Chem. Eng. Res. Des. 90 (2012) 1979–1988.
[140] H. Luo, W. Deng, J. Gao, W. Fan, G. Que, Energy Fuel 25 (2011) 1161–1167.
[141] M.P. Pileni, I. Lisiecki, Colloid Surf. A 80 (1993) 63–68.
[142] Y.I. Yoon, M.W. Kim, Y.S. Yoon, S.H. Kim, Chem. Eng. Sci. 58 (2003) 2079–2087.
[143] H. Rezaei, S.J. Ardakani, K.J. Smith, Energy Fuel 26 (2012) 2768–2778.
[144] J. Thompson, A. Vasquez, J.M. Hill, P. Pereira-Almao, Catal. Lett. 123 (2008) 16–23.
[145] D. Liu, W. Cui, Z. Shuyi, G. Que, Energy Fuel 22 (2008) 4165–4169.
[146] K.P. Tian, A.R. Mohamed, S. Bhatia, Fuel 77 (1998) 1221–1227.
[147] B. Fixari, S. Peureux, J. Elmouchnino, P. Le Perchecet, Energy Fuel 8 (1994) 588–592.
[148] C. Ovalles, E. Filgueira, A. Morales, C.E. Scott, F. Gonzalez-Gimenez, B.P. Embaid, Fuel 82 (2003) 887–892.
[149] C. Jian, L. Yihong, L. Yunhua, Q. Guohe, Petrol. Sci. Technol. 23 (2005) 1453–1462.